
Residual Connections and Normalization Can Provably Prevent Oversmoothing in GNNs

Michael Scholkemper*

Department of Computer Science
RWTH Aachen University
scholkemper@cs.rwth-aachen.de

Xinyi Wu*

Institute for Data, Systems, and Society
Massachusetts Institute of Technology
xinyiwu@mit.edu

Ali Jadbabaie

Institute for Data, Systems, and Society
Massachusetts Institute of Technology
jadbabai@mit.edu

Michael T. Schaub

Department of Computer Science
RWTH Aachen University
schaub@cs.rwth-aachen.de

Abstract

Residual connections and normalization layers have become standard design choices for graph neural networks (GNNs), and were proposed as solutions to the mitigate the oversmoothing problem in GNNs. However, how exactly these methods help alleviate the oversmoothing problem from a theoretical perspective is not well understood. In this work, we provide a formal and precise characterization of (linearized) GNNs with residual connections and normalization layers. We establish that (a) for residual connections, the incorporation of the initial features at each layer can prevent the signal from becoming too smooth, and determines the subspace of possible node representations; (b) batch normalization prevents a complete collapse of the output embedding space to a one-dimensional subspace through the individual rescaling of each column of the feature matrix. This results in the convergence of node representations to the top- k eigenspace of the message-passing operator; (c) moreover, we show that the centering step of a normalization layer — which can be understood as a projection — alters the graph signal in message-passing in such a way that relevant information can become harder to extract. We therefore introduce a novel, principled normalization layer called GraphNormv2 in which the centering step is learned such that it does not distort the original graph signal in an undesirable way. Experimental results confirm the effectiveness of our method.

1 Introduction

In recent years, graph neural networks (GNNs) have gained significant popularity due to their ability to process complex graph-structured data and extract features in an end-to-end trainable fashion [5, 12, 14, 21, 30, 38, 43]. They have shown empirical success in a highly diverse set of problems [4, 8, 27, 34, 45, 48]. Most GNNs follow a message-passing paradigm [20], where node representations are learned by recursively aggregating and transforming the representations of the neighboring nodes. Through repeated message-passing on the graph, the graph information is implicitly incorporated.

A prevalent problem in message-passing GNNs is their tendency to oversmooth [7, 29, 36, 46], which refers to the observation that node signals (or representations) tend to contract to a one-dimensional subspace as the number of layers increases. While a certain amount of smoothing is desirable

*Both authors contributed equally.

to average out noise in the node features and render information extraction from the graph more reliable [29, 47], excessive smoothing leads to an information loss as node signals become virtually indistinguishable and can thus not be exploited for downstream tasks. For this reason, most GNN architectures use only few message-passing layers [30, 43, 48]. This contrasts with the trend in deep learning, where much deeper architectures are considered preferable [24, 28].

To mitigate the oversmoothing problem for GNNs, several practical solutions have been proposed. In particular, both residual connections [9, 31] and normalization layers [22, 52, 53] have been specifically proposed to address the oversmoothing problem. Despite empirical observations that the introduction of these methods can alleviate oversmoothing and enable deeper architectures, a theoretical analysis on the effects of these methods on oversmoothing and the resultant expressive power of GNNs is still lacking. More technically, the analysis of oversmoothing typically relies on a single node similarity measure as a description of the whole underlying system [6, 36, 46]. Such measures, however, can only identify a complete collapse of the node signals to one-dimensional subspace and are unable to capture the more refined geometry of the system beyond a complete collapse. These observations motivate the following questions:

How do residual connections and normalization layers affect oversmoothing and therefore the practical expressive power of GNNs? How do they compare?

In this work, we answer the above questions with a refined characterization of the underlying system of linearized GNNs [29, 47] with residual connections and normalization layers. In particular, we establish that both methods can alleviate oversmoothing by preventing node signals from a complete collapse to a one-dimensional subspace, which is the case for standard GNNs [6, 36, 46].

Our contributions can be summarized as follows:

- We characterize the system of linearized GNNs with residual connections. We show that residual connections prevent complete rank collapse to a one-dimensional subspace by incorporating the initial features at each step. As a result, the subspace of possible node representations that a GNN can compute is determined by the initial features.
- We analyze the system of linearized GNNs with normalization layers and show that normalization layers prevent oversmoothing of node signals through the scaling step. Nonetheless, the node representations exponentially converge to the top- k eigenspace of the message-passing operator.
- We separately identify the role of the centering step in normalization layers. Our results suggest that the centering step can distort the message-passing in undesired ways. Consequently, relevant graph information becomes damped and can even be lost in message-passing.
- Based on these theoretical findings, we propose a novel normalization layer named GraphNormv2 that learns a centering operation that does not distort the subspaces of the message-passing operator in an uncontrolled way, but contains a learnable projection. Experimental results show the effectiveness of our proposed method.

2 Related Work

Oversmoothing in GNNs Oversmoothing is a known challenge for developing deeper and more powerful GNNs, and many techniques have been proposed to mitigate the issue in practice. Among them, residual connections [9] and normalization layers [22, 52, 53] are popular methods that have empirically been shown to mitigate oversmoothing to certain extent. While many theoretical works on the underlying mechanism of oversmoothing exist [7, 29, 36, 46, 47], these studies focus on standard GNNs without these additional modules. It is thus still an open question how residual connections and normalization can mitigate oversmoothing and subsequently affect the practical expressive power of GNNs from a theoretical perspective.

Theoretical studies on residual connections and normalization in deep learning The empirical success of residual connections and normalization in enhancing training deep neural networks has inspired research into their underlying mechanisms [1, 11, 18, 23, 33, 49]. Specifically, it has been shown that batch normalization avoids rank collapse for randomly initialized deep linear networks [10] and that residual connections alleviate rank collapse in transformers [13]. Rank collapse of node representations due to oversmoothing has also been a notable issue in building deeper GNNs. However, a theoretical analysis of how residual connections and normalization layers combat oversmoothing and their additional effects on message-passing in GNNs is still lacking.

3 Notation and Preliminaries

Notation We use the shorthand $[n] := \{1, \dots, n\}$. We denote the zero-vector by $\mathbf{0}$, the all-one vector by $\mathbf{1}$ and the identity matrix by I . Let $\|\cdot\|_2$, $\|\cdot\|_F$ be the 2-norm and Frobenius norm, respectively. Lastly, for a matrix M , we denote its i^{th} row by $M_{i,:}$ and j^{th} column by $M_{:,j}$.

Graph Neural Networks Most message-passing GNN models — which we will simply refer to as GNNs from now on — can be described by the following update equation:

$$X^{(t+1)} = \sigma(AX^{(t)}W^{(t)}), \quad (1)$$

where $X^{(t)}, X^{(t+1)} \in \mathbb{R}^{n \times k}$ are the input and output node representations of the t^{th} layer, respectively; $\sigma(\cdot)$ is an element-wise non-linearity such as the ReLU function; $W^{(t)} \in \mathbb{R}^{k \times k}$ is a learnable linear transformation and $A \in \mathbb{R}_{\geq 0}^{n \times n}$ represents a message-passing operation and reflects the graph structure. For example, if A is the graph adjacency matrix, $A = A_{\text{adj}}$ we recover the Graph Isomorphism Network (GIN) [48], and for $A = D^{-\frac{1}{2}}A_{\text{adj}}D^{-\frac{1}{2}}$, where $D = \text{diag}(A_{\text{adj}}\mathbf{1})$ is the diagonal degree matrix, we obtain a Graph Convolutional Network (GCN) [30].

Throughout the paper, we assume A to be symmetric and non-negative. Furthermore, we assume that eigenvalues λ_i of a matrix are organized in a non-increasing order in terms of absolute value: $|\lambda_1| \geq |\lambda_2| \geq \dots \geq |\lambda_n|$.

Normalization Layers Normalization has been believed to be beneficial to deep neural networks for nearly two decades [32]. Most normalization layers perform a *centering* operation and a *scaling* operation on the input features. Centering usually consists of subtracting the mean, centering the features around zero along the chosen dimension. Scaling usually consists of scaling the features such that the features along the chosen dimension have unit variance. The two most popular approaches are *batch* and *layer* normalization [2, 26]. In our work, we focus on batch normalization (BatchNorm), denoted as $\text{BN}(\cdot)$, which is defined as follows: Let $X \in \mathbb{R}^{n \times k}$, then

$$\text{BN}(X) = [\dots, \text{bn}(X_{:,i}), \dots],$$

where $\text{bn}(x) = (x - \sum_{i=1}^n x_i/n) / \|x - \sum_{i=1}^n x_i/n\|_2$. We note that in the case of GNNs, especially graph classification tasks, batches may contain nodes from different graphs. In our analysis, we consider only the nodes in the same graph for normalization and nodes in different graphs do not influence each other. This is sometimes called *instance* normalization [42].

GraphNorm In Cai et al. [7], the authors proposed GraphNorm, a normalization layer specifically designed for GNNs that is like BatchNorm in terms of acting on the columns of the feature matrix. Nonetheless, compared to BatchNorm, instead of subtracting the mean, the method learns to subtract an τ_j portion of the mean for the j^{th} column:

$$\text{GraphNorm}(X_{:,j}) = \gamma_j \frac{X_{:,j} - \tau_j \mathbf{1} \mathbf{1}^\top X_{:,j} / n}{\sigma_j} + \beta_j,$$

where $\sigma_j = \|X_{:,j} - \tau_j \mathbf{1} \mathbf{1}^\top X_{:,j} / n\|_2 / \sqrt{n}$, γ_j, β_j are the learnable affine parameters as in the implementation of other normalization methods [2, 26]. Notably, by introducing τ_j for each feature dimension j , [7] claims an advantage of GraphNorm over the original batch normalization in that GraphNorm is able to learn how much of the information to keep in the mean rather than always subtracting the entire mean away.

Weisfeiler-Leman and Structural Eigenvectors In theoretical studies about GNNs, an algorithm that comes up frequently is the so-called Weisfeiler-Leman (WL) algorithm [44]. This algorithm iteratively assigns a color $c(v) \in \mathbb{N}$ to each node v starting from a constant initial coloring $c^{(0)}(v) = 1$ for all nodes. In each iteration, an update of the following form is computed: $c^{(t+1)}(v) = \text{hash}(c^{(t)}(v), \{\{c^{(t)}(x) \mid x \in \mathcal{N}(v)\}\})$, where hash is an injective hash function, $\{\{\cdot\}\}$ denotes a multiset in which elements can appear more than once, and $\mathcal{N}(v)$ is the set of neighboring nodes of v . The algorithm returns the final colors $c^{(\infty)}$ when the partition $\{(c^{(t)})^{-1}(c^{(t)}(v)) \mid v\}$ no longer changes for consecutive update t . For GNNs, Morris et al. [34] and Xu et al. [48] have showed that for graphs with constant initial node features, GNNs cannot compute different features for nodes that are in the same class in the final coloring $c^{(\infty)}$.

For this paper, an equivalent algebraic perspective of the WL algorithm² will be more useful (see Appendix A.1 for a detailed discussion): Given $c^{(\infty)}$ with $\text{Im}(c^{(\infty)}) = \{c_1, \dots, c_k\}$, define $H \in \{0, 1\}^{n \times k}$ such that $H_{v,i} = 1$ if and only if $c^{(\infty)}(v) = c_i$. It holds that

$$AH = HA^\pi, \quad (2)$$

where $A^\pi \in \mathbb{R}^{k \times k}$ is the adjacency matrix of the *quotient graph*, which is fixed given A and H . In words, a node in the quotient graph represents a class of nodes in the original graph who share the same number of neighbors in each final color.

Most relevantly, the adjacency matrix A of the original graph inherits all the eigenpairs from the quotient graph: If ν^π is the eigenvector of A^π with eigenvalue λ , then $H\nu^\pi$ is an eigenvector of A with eigenvalue λ . We call such eigenvectors of A the *structural eigenvectors*. These eigenvectors are important for understanding dynamical systems on graphs [39, 51], and play a role for centrality measures such as PageRank [37] and others [41]. In fact, from the results of Morris et al. [34] and Xu et al. [48], we can directly infer that given constant initial features, GNNs effectively compute node features on this quotient graph, meaning the features lie in the space spanned by the structural eigenvectors.

4 Main Results: Defying Oversmoothing

Both residual connections and normalization methods are commonly used to mitigate oversmoothing [9, 22, 31, 52, 53]. In this section, we show that these methods in fact *provably* prevent oversmoothing. We further analyze what implications the use of these methods has for the underlying system of GNNs.

Consider the following node similarity measure [36, 46], which is a common metric in the literature to detect oversmoothing:

$$\mu(X) := \|X - \mathbf{1}\mathbf{1}^\top X/n\|_F = \|(I - \mathbf{1}\mathbf{1}^\top/n)X\|_F. \quad (3)$$

$\mu(X)$ equals zero if and only if all the columns of X collapse to the one-dimensional subspace where all nodes have the same value. In Wu et al. [46], oversmoothing is defined to be the case where $\mu(X^{(t)}) \rightarrow 0$ as $t \rightarrow \infty$ and the authors show that oversmoothing happens exponentially for random walk GCNs and more general attention-based GNNs. Meanwhile, Cai et al. [7], Oono and Suzuki [36] establish a similar result for standard GCNs stating that node signals converge to the dominant eigenspace of the message-passing operator $D^{-\frac{1}{2}}A_{\text{adj}}D^{-\frac{1}{2}}$ by using a variant of $\mu(\cdot)$. These results suggest that for all such GNNs with non-diverging weights, complete collapse of node signals to a one-dimensional subspace occurs after repeated message-passing, irrespective of the initial features. However, we will show below that these results do not hold for GNNs with residual connections or BatchNorm.

For the following theoretical analysis, we investigate a linearized GNN, meaning that $\sigma(\cdot)$ is the identity map. For simplicity, we assume, if not specified otherwise, that the weights $(W_1^{(t)})_{i,j}, (W_2^{(t)})_{i,j}, W_{i,j}^{(t)}$ are randomly sampled i.i.d. Gaussians, which is typical for GNNs before training. Such a setting is relevant in practice as oversmoothing is present in GNNs before training has started, making the gradients used for back propagation almost vanish and training of the network becomes much harder. Yet, most results hold under more general conditions. The complete proofs of all the results in the main text and the results under general conditions are provided in Appendix B.

4.1 Residual Connections Prevent Complete Collapse

For our analysis of residual connections, we focus on the commonly used initial residual connections, which are deployed, e.g., in GCNII [9]. Such residual connections are closely related to the Personalized PageRank propagation [31]. For generality, we write the unified layer-wise update rule for both methods as follows:

$$X^{(t+1)} = (1 - \alpha)AX^{(t)}W_1^{(t)} + \alpha X^{(0)}W_2^{(t)}, \quad (4)$$

²This algebraic characterisation is also known as the *coarsest equitable partition* (*cEP*) of the graph.

where $\alpha X^{(0)}$ corresponds to the initial residual connection, and $\alpha \in (0, 1)$ can be seen as the strength of residual connections or alternatively as the teleportation probability in the Personalized PageRank Propagation. Note that for the Personalized PageRank Propagation method (APPNP) proposed in [31], $A = D^{-\frac{1}{2}} A_{\text{adj}} D^{-\frac{1}{2}}$, $W_1^{(t)} = I_k$ for all $t \geq 0$.

Intuitively, compared to the case for standard message-passing GNNs in (1), at each update step, a linear combination of the residual signal $\alpha X^{(0)}$ is now added to the features. As long as the weight matrices are not chosen such that they annihilate the residual signal, this will prevent the features from collapsing to a smaller subspace. This implies that $\mu(X^{(t)})$ would be strictly greater than zero.

Proposition 4.1. *If $\mu(X^{(0)}) > 0$, then $\mu(X^{(t)}) > 0$ with probability 1.*

The above result suggests that, with proper initialization of node features, initial residual connections will alleviate oversmoothing almost surely, meaning the features will not be smooth after iterative message-passing at initialization. Nonetheless, it is worth noting that the node similarity measure $\mu(X)$ can only identify a complete collapse to a one-dimensional subspace, where all nodes share the same representation vector, in which case $\mu(X)$ equals zero. Even if $\mu(X)$ can remain strictly positive with residual connections, this does not eliminate the possibility that there may still be partial collapse of the signal to a lower-dimensional subspace. However, as we will show with the following result, with residual connections (4), no such partial collapse occurs.

Proposition 4.2. *Let $x_i = X_{:,i}^{(0)}$ and let $\|x_i\|_2 = 1$ for $i \in [k]$. Let each $(W_l^{(t)})_{y,z} \stackrel{\text{i.i.d.}}{\sim} \mathcal{N}(\eta, s^2)$. Then for any $\epsilon > 0$, $\|x_i^\top X^{(t)}\|_2 \geq \epsilon$ with probability at least $p = 1 - \exp\left(-\frac{\epsilon^2}{2\alpha^2 s^2}\right)$.*

This result essentially says that a part of the initial signal is maintained after each layer with high probability. We can further give a more refined characterization of what node features the system in (4) can compute after repeated rounds of message-passing.

Proposition 4.3. *Let $\text{Kr}(A, X^{(0)}) = \text{Span}(\{A^{i-1} X_{:,j}^{(0)}\}_{i \in [n], j \in [k]})$ be the Krylov subspace. Let $Y \in \mathbb{R}^{n \times k}$. Then there exist a $T \in \mathbb{N}$ and sequence of weights $W_1^{(0)}, W_2^{(0)}, \dots, W_1^{(T-1)}, W_2^{(T-1)}$ such that $X^{(T)} = Y$ if and only if $Y \in \text{Kr}(A, X^{(0)})$.*

The result shows that for a message-passing GNN with residual connections, the subspace that the embedding $X^{(t)}$ lies in is governed by the initial features $X^{(0)}$ together with the message-passing operator A and that any such signal is reachable by a sequence of weights. This is in contrast with the behavior of standard message-passing GNNs, for which node representations eventually becomes “memoryless”, i.e., independent of initial features. In particular, for standard GCNs, the subspace the system converges to is completely governed by the message-passing operator A [36].

Remark 4.4. Our results also suggest that whether initial residual connections would work for oversmoothing heavily depends on the initialization of features. If chosen poorly, they may not be able to prevent oversmoothing. In particular, a constant initialization of features is unhelpful to prevent oversmoothing with initial residual connections.

4.2 BatchNorm Prevents Complete Collapse

Having discussed the effect of residual connections, in this section, we switch gears and analyze how BatchNorm affects GNNs. We consider the following combination of GNNs with BatchNorm:

$$X^{(t+1)} = \text{BN}(Y^{(t+1)}), \quad Y^{(t+1)} = \sigma(AX^{(t)}W^{(t)}). \quad (5)$$

Similar to the analysis on GNNs with initial residual connections, we will show that BatchNorm prevents complete collapse of the output embedding space to the all-ones subspace. We again consider the case where $\sigma(\cdot)$ is the identity map. Note that even though the GNN computation is now linearized, the overall system remains non-linear because of the BatchNorm operation. Let us consider now $V_{\neq 0} \in \mathbb{R}^{n \times k'}$ to be the matrix of eigenvectors associated to non-zero eigenvalues of $(I_n - \mathbf{1}\mathbf{1}^\top/n)A$.

Proposition 4.5. *Let $\text{Rank}(V_{\neq 0}^\top X^{(0)}) > 1$, then $\mu(X^{(t)}) \geq \sqrt{2}$ for all $t \geq 1$ with probability 1.*

The above result suggests that with BatchNorm, $\mu(X^{(t)})$ can be maintained strictly greater than a nontrivial constant at each layer, indicating that complete collapse to the all-ones subspace does

not happen. Notably, a generalized result also holds for the case where $W^{(t)}$ is the identity matrix for all $t \geq 0$, meaning that the corresponding system does not oversmooth in terms of $\mu(\cdot)$ with BatchNorm (see Appendix B.6). This again, stands in contrast to the case in standard GNNs without BatchNorm, in which having $W^{(t)} = I_k$ has been proven to oversmooth in GCNs and more general attention-based GNNs [36, 46].

Remark 4.6. A more general version of the above result holds for both linear and non-linear GNNs, when assuming $\sigma(\cdot)$ is injective: $\mu(X^{(t)}) = \sqrt{k}$ for all $t \geq 1$, where k is the hidden dimension of features. See Appendix B.7 for a detailed discussion. If nonlinearity $\sigma(\cdot)$ is applied after BatchNorm, then it also holds that $\mu(X^{(t)}) > 0$ for all $t \geq 1$ under proper assumptions. See Appendix B.8 for a detailed discussion.

However, as what we have discussed for the case of residual connections, the node similarity measure $\mu(X)$ can only capture complete collapse to a one-dimensional subspace. In what follows, we will provide a more precise characterization of the convergence behaviors of GNNs with BatchNorm. Notably, since the scaling operation of BatchNorm guarantees that the system will not diverge or collapse, we can give an exact asymptotic characterization. Let $V_k \in \mathbb{R}^{n \times k}$ be the matrix of the top- k eigenvectors of $(I_n - \mathbf{1}\mathbf{1}^\top/n)A$. We will show that the resulting linearized GNN converges to a rank- k subspace spanned by the top- k eigenvectors of $(I_n - \mathbf{1}\mathbf{1}^\top/n)A$.

Proposition 4.7. Suppose $V_k^\top X^{(0)}$ has rank k , then for all weights $W^{(t)}$, the GNN with BatchNorm given in (5) exponentially converges to the column space of V_k .

In the proof of Proposition 4.7, it becomes clear that the centering operation in BatchNorm is the reason for which we use the *centered* message-passing operator $(I_n - \mathbf{1}\mathbf{1}^\top/n)A$. If we left out the centering step and only keep the scaling step of BatchNorm, the proof would work in the same way (switching all occurrences of $(I_n - \mathbf{1}\mathbf{1}^\top/n)A$ with A). This implies that the *column-wise scaling operation is responsible for the preservation of the rank of the features*. Furthermore, there are no requirements for the weights as in the case without BatchNorm [36, 46]: even extremely large or random weights can be chosen, as the scaling ensures that the system neither diverges nor collapses.

Moreover, the convergence of the linearized system in (5) to a k -dimensional subspace can be shown to be tight: we can choose weights such that the top- k eigenvectors are exactly recovered. This is of course only possible if these eigenvectors do have a nonzero eigenvalue, which we assume for the result below, in that, none of the top- k eigenvectors of $(I_n - \mathbf{1}\mathbf{1}^\top/n)A$ has eigenvalue $\hat{\lambda}_i$ zero.

Proposition 4.8. Suppose $|\hat{\lambda}_k| > 0$ and $V_k^\top X^{(0)}$ has rank k . For any $\epsilon > 0$, there exists $T > 0$ and a sequence of weights $W^{(0)}, W^{(1)}, \dots, W^{(T)}$ such that for all $t \geq T$ and $i \in [k]$,

$$\left\| \nu_i^\top X_{:,i}^{(t)} \right\|_2 \geq 1/\sqrt{1+\epsilon},$$

where ν_i denotes the i -th eigenvector of $(I_n - \mathbf{1}\mathbf{1}^\top/n)A$.

In fact, the above result ties in nicely with recent results showing that GNNs are strengthened through *positional encodings* [15, 16], where the features are augmented by the top- k eigenvectors of the graph. This can, in some sense, be seen as emulating a deep GNN, which would converge to the top- k eigenspace using BatchNorm. Yet it is worth noting that while BatchNorm improves the practical expressive power of GNNs by converging to a larger subspace, under the type of convergence given in Proposition 4.7, the information in the eigenvectors associated with small magnitude eigenvalues is still damped after repeated message-passing.

Remark 4.9. If no initial node features $X^{(0)}$ are given by the dataset, common choices in practice are to initialize the features randomly or identically for each node. In the former case, the prerequisites of 4.7 and Proposition 4.8 are satisfied. In the latter case, the conditions are not met, as $X^{(0)}$ has rank one. In that case, the system still converges. In fact, it retains its rank and converges to the dominant eigenvector of $(I_n - \mathbf{1}\mathbf{1}^\top/n)A$.

4.3 Comparison between normalization and residual connections

From previous sections, we have seen that both residual connections and batch normalization are able to prevent a complete collapse of the node embeddings to a one-dimensional subspace. In both cases, the embeddings converge to a larger subspace and thus oversmoothing is alleviated. However, it is

clear that different mechanisms are at play to mitigate oversmoothing. With residual connections, the system is able to keep the dimensions of the initial input features by incorporating the initial features $X^{(0)}$ at each layer; while with normalization, the system converges to the subspace of the top eigenvectors of the message-passing operator through the scaling step.

5 Centering Distorts the Graph

So far, we have analyzed the effects of residual connections and normalization layers on oversmoothing. Specifically, we have shown that the incorporation of initial features of residual connections and the scaling effect of normalization help alleviate complete rank collapse of node features. However, there are two steps in normalization layers: centering and scaling. If already scaling helps preventing a complete collapse, a natural question is *what is the role of centering in the process?* In this section, we will show that the current centering operation used in normalization layers can in fact have an undesirable effect altering the graph signal that message-passing can extract, as if message-passing happens on a different graph.

5.1 Centering Interferes the Structural Eigenvectors

The centering operation in normalization layers takes away the (scaled) mean across all rows in each column, and thus can be written as applying the operator $I_n - \tau \mathbf{1} \mathbf{1}^\top / n$ to the input, where τ indicates how much mean is taken away in centering. Specifically, for $\tau = 1$ we recover BatchNorm, whereas for $\tau \in \mathbb{R}$, we recover GraphNorm [7]. To analyze how this step would alter the graph signal message-passing can extract, we make use of the concepts of quotient graph and structural eigenvectors as introduced in Section 3.

Given a symmetric, non-negative adjacency matrix $A \in \mathbb{R}_{\geq 0}^{n \times n}$, let $H \in \{0, 1\}^{n \times m}$ be the indicator matrix of its final WL coloring $c^{(\infty)}$. Consider the eigenpairs $\mathcal{V} = \{..., (\lambda, \nu), ...\}$ of A and divide them into the set of structural eigenpairs $\mathcal{V}_{\text{struc}} = \{(\lambda, \nu) \in \mathcal{V} \mid \nu = H \nu^\pi\}$, and the remaining eigenpairs $\mathcal{V}_{\text{rest}} = \mathcal{V} \setminus \mathcal{V}_{\text{struc}}$. Similarly, let $\hat{\mathcal{V}} = \{..., (\hat{\lambda}, \hat{\nu}), ...\}$ be the eigenpairs of $(I_n - \tau \mathbf{1} \mathbf{1}^\top / n)A$. We now analyze what happens to these distinct sets of eigenvectors when applying the centering operation. Notice that the parameter τ controls how much of the mean is taken away and thus how much the centering influences the input graph. However, *as long as τ is not zero, there is always an effect altering the graph operator used in message-passing*:

Proposition 5.1. *Assuming $\tau \neq 0$,*

1. $\mathcal{V}_{\text{rest}} \subset \hat{\mathcal{V}}$.
2. *Assume that A is not regular, then the dominant eigenvector ν of A is **not** an eigenvector in $\hat{\mathcal{V}}$ for any eigenvalue.*
3. $\sum_{(\lambda, \nu) \in \mathcal{V}_{\text{struc}}} \lambda > \sum_{(\hat{\lambda}, \hat{\nu}) \in \hat{\mathcal{V}} \setminus \mathcal{V}_{\text{rest}}} \hat{\lambda}$.

Here, we consider a general case where the graph is not regular, meaning there is more than one color in the final WL coloring $c^{(\infty)}$. Assuming constant initialization of node features, $\mathcal{V}_{\text{struc}}$ spans the space of all possible node features that a GNN can compute and Proposition 5.1 states that it is exactly the space that the centering acts on. Specifically, while leaving the eigenvectors and eigenvalues in $\mathcal{V}_{\text{rest}}$ untouched, centering changes the eigenvector basis of the space spanned by $\mathcal{V}_{\text{struc}}$ in two ways: some vectors, such as the dominant eigenvector, are affected by this transformation and thus no longer convey the same information. At the same time, the centering transformation may change the magnitude of eigenvalues — that is, the dominant eigenvector may not be dominant anymore. Meanwhile, the whole space is pushed downward in the spectrum, meaning that after the centering transformation, the signal components within the structural eigenvectors are damped and thus become less pronounced in the node representations given by the GNN.

Notably, such an effect altering the graph signal not only applies to BatchNorm with $\tau = 1$, but also GraphNorm [7], which was proposed specifically for GNNs. In their paper, the authors address the problem that BatchNorm’s centering operation completely nullifies the graph signal on regular graphs. Their remedy is to only subtract an τ portion of the mean instead. However, Proposition 5.1 shows that a similar underlying problem altering the graph signal would persist for general graphs even switching from BatchNorm to GraphNorm.

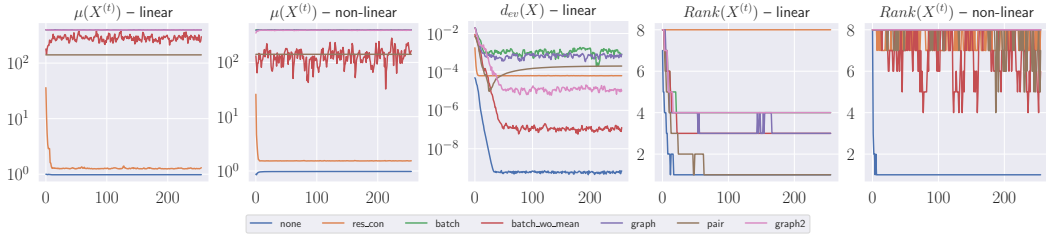


Figure 1: **Long Term behavior of GCN.** Progression of $\mu(X^{(t)})$ and $\text{Rank}(X^{(t)})$ over 256 iterations of message-passing in both linear and non-linear GCN. In the linear case, $\mu(X^{(t)})$ remains constant for all methods, indicating that complete collapse to the all-ones space does not happen. However, PairNorm and the non-normalized variant do collapse in terms of rank, while the other methods maintain a rank greater than 2. All the phenomena are explained by our theory. In the non-linear case, the models behave similarly. Notably, centering seems to prevent rank collapse in the non-linear case as PairNorm no longer collapses in rank.

Comparison with standard neural networks The use of normalization techniques in GNNs was inspired by use of normalization methods in standard feed-forward neural networks [26]. Here, we want to emphasize that the issue centering causes in GNNs as described above is not a problem for standard neural networks, as standard neural networks do not need to incorporate the graph information in the forward pass. As a result, in standard neural networks, normalization transforms the input in a way that it does not affect the classification performance: for each neural network, there exists a neural network that yields an equivalent classification after normalization. However, this is not the case for GNNs. In GNNs, the graph information is added in through message-passing, which can be heavily altered by normalization as shown above. Such normalization can lead to information loss, negatively impacting the model’s performance.

5.2 Our Method: GraphNormv2

Based on our theoretical analysis, we propose a new normalization layer for GNNs which has a similar motivation as the original GraphNorm but improves the centering operation to not affect the graph information in message-passing. Specifically, instead of naive centering, which can be thought of as subtracting a projection to the all-ones space, we use a learned projection. Learning a completely general projection may have certain downsides, however. As graphs can have different sizes, we either would need to learn different projections for different graph sizes or use only part of the learned projection for smaller graphs. We thus opt for learning a centering that transforms the features by subtracting an $(\tau_j)_i$ portion of the i -th eigenvector from the j -th column. Our proposed graph normalization is thus:

$$\text{GraphNormv2}(X_{:,j}) = \gamma_j \frac{X_{:,j} - (V_{k+} \tau_j \tau_j^\top V_{k+}^\top) X_{:,j}}{\sigma_j} + \beta_j,$$

where $\tau_j \in \mathbb{R}^{k+1}$ is a learnable parameter, $\sigma_j = \|X_{:,j} - (V_{k+} \tau_j \tau_j^\top V_{k+}^\top) X_{:,j}\|_2$, and γ_j, β_j are the learnable affine parameters. Instead of just using the top- k eigenvectors V_k of the message-passing operator, we use V_k and one additional vector $r = \mathbf{1} - V_k V_k^\top \mathbf{1}$ that guarantee one to retrieve the all-ones vector $\mathbf{1}$. We denote the set $V_{k+} := V_k \cup \{r\}$. This ensures backward compatibility, in that, GraphNormv2 can emulate GraphNorm and BatchNorm.

6 Numerical Experiments

In this section, we investigate the benefits that can be derived from the proposed graph normalization method GraphNormv2. We examine the long term behavior of linear and non-linear GNNs by conducting an ablation study on randomly initialized, untrained GNNs. We then go on to inspect the practical relevance of our proposed method. More details about the experiments are provided in Appendix C.

Rank collapse in linear and non-linear GNNs We investigate the effect of normalization in deep (linear) GNNs on the Cora dataset [50]. We employ seven different architectures: an architecture using residual connections, BatchNorm [26], BatchNorm without the centering operation, PairNorm [52],

Table 1: Performance under different normalization layers. Performance of GIN, GCN, and GAT with different normalization layers on graph classification task (MUTAG, PROTEINS, and PTC-MR) and node classification task (Cora, CiteSeer, and ogbn-arxiv). Results are reported as the mean accuracy (in %) \pm std. over 10 independent trials and 5 folds. Best results are highlighted in blue; second best results are highlighted in gray.

		Graph Classification			Node Classification			Node Classification (# layers=20)	
		MUTAG	PROTEINS	PTC-MR	Cora	CiteSeer	ogbn-arxiv	Cora	CiteSeer
GCN	no norm	78.2 \pm 7.8	70.5 \pm 4.0	57.7 \pm 3.0	82.6 \pm 4.6	89.4 \pm 0.6	67.4 \pm 0.2	46.0 \pm 11.5	65.6 \pm 4.3
	batch	81.5 \pm 2.0	70.4 \pm 1.8	56.0 \pm 3.5	85.2 \pm 0.6	89.4 \pm 0.7	68.3 \pm 0.3	84.0 \pm 1.6	82.2 \pm 4.4
	graph	81.1 \pm 4.7	71.4 \pm 3.6	58.1 \pm 4.8	85.1 \pm 0.8	89.1 \pm 0.7	68.3 \pm 0.2	80.5 \pm 6.3	82.7 \pm 2.1
	pair	61.3 \pm 10.1	59.6 \pm 0.0	55.8 \pm 0.0	84.2 \pm 0.7	88.2 \pm 0.7	63.0 \pm 1.2	82.3 \pm 0.5	74.0 \pm 14.1
	graphv2	82.6 \pm 4.6	72.6 \pm 2.6	56.5 \pm 4.8	85.8 \pm 0.5	89.5 \pm 0.6	68.3 \pm 0.3	84.8 \pm 0.8	83.4 \pm 2.0
GAT	no norm	78.5 \pm 5.3	71.2 \pm 2.0	61.3 \pm 4.2	85.9 \pm 0.9	93.7 \pm 0.5	68.3 \pm 0.9	79.2 \pm 0.7	89.1 \pm 0.5
	batch	82.5 \pm 4.1	68.4 \pm 5.2	55.7 \pm 0.7	86.2 \pm 0.7	94.9 \pm 0.5	71.0 \pm 0.1	85.8 \pm 0.7	94.2 \pm 0.6
	graph	81.2 \pm 4.8	71.9 \pm 2.4	60.3 \pm 5.4	86.3 \pm 0.9	94.8 \pm 0.5	71.0 \pm 0.1	85.7 \pm 0.8	94.0 \pm 0.6
	pair	59.7 \pm 11.1	60.1 \pm 0.9	55.7 \pm 1.1	85.4 \pm 1.0	93.4 \pm 1.2	70.0 \pm 0.2	84.9 \pm 0.7	92.5 \pm 1.0
	graphv2	81.6 \pm 3.8	71.0 \pm 2.6	59.5 \pm 4.4	86.3 \pm 0.8	94.8 \pm 0.5	70.9 \pm 0.2	85.7 \pm 0.8	94.4 \pm 0.5
GIN	no norm	79.7 \pm 5.9	70.7 \pm 3.6	59.2 \pm 3.9	33.4 \pm 45.4	47.0 \pm 3.1	21.6 \pm 0.0	28.2 \pm 6.2	23.4 \pm 5.1
	batch	82.5 \pm 5.0	69.2 \pm 5.3	52.9 \pm 5.3	68.4 \pm 4.0	49.7 \pm 6.8	21.1 \pm 7.9	31.4 \pm 5.4	23.6 \pm 6.1
	graph	83.7 \pm 4.2	72.6 \pm 2.4	59.1 \pm 5.1	33.2 \pm 3.4	63.0 \pm 11.0	21.6 \pm 0.0	26.9 \pm 5.2	27.1 \pm 4.6
	pair	65.2 \pm 3.2	64.5 \pm 4.3	55.5 \pm 1.6	37.2 \pm 3.5	51.1 \pm 9.2	20.7 \pm 9.6	28.6 \pm 6.2	26.9 \pm 4.7
	graphv2	84.9 \pm 3.6	71.0 \pm 3.6	60.1 \pm 5.5	86.5 \pm 0.9	94.9 \pm 0.5	68.9 \pm 0.3	83.8 \pm 2.0	93.8 \pm 0.7

GraphNorm [7], GraphNormv2, and finally no normalization as a baseline. Each of these methods is used in an untrained, randomly initialized GCN [30] (without biases) with 256 layers.

We compare these models using the following measures of convergence: $\mu(X^{(t)})$ as defined in (3), the eigenvector space projection: $d_{\text{ev}}(X) := \frac{1}{n} \|X - VV^\top X\|_F$, where $V \in \mathbb{R}^{n \times n}$ is the set of normalized eigenvectors of A , and the numerical rank of the features $\text{Rank}(X^{(t)})$. The results are shown in Figure 1. The same experiment with both GIN and GAT can be found in the appendix together with additional measures of convergence.

The two left panels of Figure 1 show that the commonly considered metric for measuring over-smoothing $\mu(X)$ indeed does not detect any collapse of the feature space — neither in the linear nor non-linear case. However, the right two panels show that there is more going on as PairNorm and no norm do collapse to a rank one subspace in the linear case. Specifically, they converge to the dominant eigenvector of $(I_n - \tau \mathbf{1} \mathbf{1}^\top / n) D^{-\frac{1}{2}} A D^{-\frac{1}{2}}$ and $D^{-\frac{1}{2}} A D^{-\frac{1}{2}}$, respectively, as evident from the middle panel. The other methods are able to preserve a rank greater than two over all iterations. However, they do converge to a low-dimensional subspace, e.g. GraphNormv2 converges to the top- k eigenvector space as can be seen in the middle panel. All of these phenomena are explained by our theoretical analysis. As for the non-linear case, the models behave similarly apart from two things: (a) there is no convergence to the linear subspace due to the non-linearity $\sigma(\cdot)$, although the rank can still be preserved. (b) The centering operation seems to prevent rank collapse in the non-linear case as PairNorm no longer collapses in rank.

Classification performance We evaluate the effectiveness of our method GraphNormv2 for real graph learning tasks. We perform graph classification tasks on the standard benchmark datasets MUTAG [40], PROTEINS [35] and PTC-MR [3] as well as node classification tasks on Cora, CiteSeer [50] and large-scale ogbn-arxiv [25]. Following the general set-up of [17], we investigate the performance of GIN, GCN and GAT in a 5-fold cross-validation setting. Details on hyperparameter tuning and other specifics can be found in Appendix C. The final test scores are obtained as the mean scores across the 5 folds and 10 independent trials with the selected hyperparameters. We then also repeat the same experiment on Cora and CiteSeer where we fix the depth of the models to 20 layers. The results are reported in Table 1.

Table 1 shows improvements on most benchmarks for our proposed normalization technique GraphNormv2. Although our method yields weak performance improvements in certain cases, this trend is apparent across datasets and tasks and even seems to be independent of the architecture. It is however worth mentioning that our method seems not to perform as well with GAT. This may be the result of GAT having both asymmetric and time-varying message-passing operators due to the attention mechanism [46] — both aspects are outside the scope of our current analysis.

7 Discussion

In this paper, we have analyzed the effect of both residual connections and normalization layers in GNNs. We show that both methods provably alleviate oversmoothing through the incorporation of the initial features and the scaling operation, respectively. In addition, by identifying that the centering operation in a normalization layer alters the graph information in message-passing, we proposed GraphNormv2, a novel normalization layer which does not distort the graph and empirically verified its effectiveness.

Our experiments showed that the trends described by our theoretical analysis are visible even in the non-linear case. Future work may concern itself with closing the gap and explaining how centering together with non-linearity can prevent node representations from collapsing to a low-dimensional subspace.

References

- [1] S. Arora, Z. Li, and K. Lyu. Theoretical analysis of auto rate-tuning by batch normalization. In *ICLR*, 2018.
- [2] J. Ba, J. R. Kiros, and G. E. Hinton. Layer normalization. *ArXiv*, abs/1607.06450, 2016.
- [3] Y. Bai, H. Ding, Y. Qiao, A. Marinovic, K. Gu, T. Chen, Y. Sun, and W. Wang. Unsupervised inductive graph-level representation learning via graph-graph proximity. In *IJCAI*, 2019.
- [4] P. Battaglia, R. Pascanu, M. Lai, D. Jimenez Rezende, and k. kavukcuoglu. Interaction networks for learning about objects, relations and physics. In *NeurIPS*, 2016.
- [5] J. Bruna, W. Zaremba, A. D. Szlam, and Y. LeCun. Spectral networks and locally connected networks on graphs. In *ICLR*, 2014.
- [6] C. Cai and Y. Wang. A note on over-smoothing for graph neural networks. In *ICML Graph Representation Learning and Beyond (GRL+) Workshop*, 2020.
- [7] T. Cai, S. Luo, K. Xu, D. He, T.-y. Liu, and L. Wang. Graphnorm: A principled approach to accelerating graph neural network training. In *ICML*, 2021.
- [8] Q. Cappart, D. Chételat, E. B. Khalil, A. Lodi, C. Morris, and P. Velickovic. Combinatorial optimization and reasoning with graph neural networks. *Journal of Machine Learning Research*, 2021.
- [9] M. Chen, Z. Wei, Z. Huang, B. Ding, and Y. Li. Simple and deep graph convolutional networks. In *ICML*, 2020.
- [10] H. Daneshmand, J. M. Kohler, F. R. Bach, T. Hofmann, and A. Lucchi. Batch normalization provably avoids ranks collapse for randomly initialised deep networks. In *NeurIPS*, 2020.
- [11] H. Daneshmand, A. Joudaki, and F. R. Bach. Batch normalization orthogonalizes representations in deep random networks. In *NeurIPS*, 2021.
- [12] M. Defferrard, X. Bresson, and P. Vandergheynst. Convolutional neural networks on graphs with fast localized spectral filtering. In *NeurIPS*, 2016.
- [13] Y. Dong, J.-B. Cordonnier, and A. Loukas. Attention is not all you need: Pure attention loses rank doubly exponentially with depth. In *ICML*, 2021.
- [14] D. K. Duvenaud, D. Maclaurin, J. Aguilera-Iparraguirre, R. Gómez-Bombarelli, T. D. Hirzel, A. Aspuru-Guzik, and R. P. Adams. Convolutional networks on graphs for learning molecular fingerprints. In *NeurIPS*, 2015.
- [15] V. P. Dwivedi, A. T. Luu, T. Laurent, Y. Bengio, and X. Bresson. Graph neural networks with learnable structural and positional representations. *arXiv preprint arXiv:2110.07875*, 2021.
- [16] V. P. Dwivedi, C. K. Joshi, A. T. Luu, T. Laurent, Y. Bengio, and X. Bresson. Benchmarking graph neural networks. *Journal of Machine Learning Research*, 24(43):1–48, 2023.

- [17] F. Errica, M. Podda, D. Bacciu, and A. Micheli. A fair comparison of graph neural networks for graph classification. *arXiv preprint arXiv:1912.09893*, 2019.
- [18] C. Esteve, B. Geshkovski, D. Pighin, and E. Zuazua. Large-time asymptotics in deep learning. *ArXiv*, abs/2008.02491, 2020.
- [19] M. Fey and J. E. Lenssen. Fast graph representation learning with PyTorch Geometric. In *ICLR Workshop on Representation Learning on Graphs and Manifolds*, 2019.
- [20] J. Gilmer, S. S. Schoenholz, P. F. Riley, O. Vinyals, and G. E. Dahl. Neural message passing for quantum chemistry. In *ICML*, 2017.
- [21] M. Gori, G. Monfardini, and F. Scarselli. A new model for learning in graph domains. In *IJCNN*, 2005.
- [22] X. Guo, Y. Wang, T. Du, and Y. Wang. Contranorm: A contrastive learning perspective on oversmoothing and beyond. In *ICLR*, 2023.
- [23] M. Hardt and T. Ma. Identity matters in deep learning. In *ICLR*, 2017.
- [24] K. He, X. Zhang, S. Ren, and J. Sun. Deep residual learning for image recognition. In *CVPR*, 2016.
- [25] W. Hu, M. Fey, M. Zitnik, Y. Dong, H. Ren, B. Liu, M. Catasta, and J. Leskovec. Open graph benchmark: Datasets for machine learning on graphs. *arXiv preprint arXiv:2005.00687*, 2020.
- [26] S. Ioffe and C. Szegedy. Batch normalization: Accelerating deep network training by reducing internal covariate shift. In *ICML*, 2015.
- [27] K. Jha, S. Saha, and H. Singh. Prediction of protein–protein interaction using graph neural networks. *Scientific Reports*, 2022.
- [28] J. Kaplan, S. McCandlish, T. J. Henighan, T. B. Brown, B. Chess, R. Child, S. Gray, A. Radford, J. Wu, and D. Amodei. Scaling laws for neural language models. *ArXiv*, abs/2001.08361, 2020.
- [29] N. Keriven. Not too little, not too much: a theoretical analysis of graph (over)smoothing. In *NeurIPS*, 2022.
- [30] T. N. Kipf and M. Welling. Semi-supervised classification with graph convolutional networks. In *ICLR*, 2017.
- [31] J. Klicpera, A. Bojchevski, and S. Günnemann. Predict then propagate: Graph neural networks meet personalized pagerank. In *ICLR*, 2019.
- [32] Y. LeCun, L. Bottou, G. B. Orr, and K.-R. Müller. Efficient backprop. In *Neural networks: Tricks of the trade*, pages 9–50. Springer, 2002.
- [33] T. Liu, M. Chen, M. Zhou, S. S. Du, E. Zhou, and T. Zhao. Towards understanding the importance of shortcut connections in residual networks. In *NeurIPS*, 2019.
- [34] C. Morris, M. Ritzert, M. Fey, W. L. Hamilton, J. E. Lenssen, G. Rattan, and M. Grohe. Weisfeiler and leman go neural: Higher-order graph neural networks. In *AAAI*, 2019.
- [35] C. Morris, N. M. Kriege, F. Bause, K. Kersting, P. Mutzel, and M. Neumann. Tudataset: A collection of benchmark datasets for learning with graphs. In *ICML Graph Representation Learning and Beyond (GRL+) Workshop*, 2020.
- [36] K. Oono and T. Suzuki. Graph neural networks exponentially lose expressive power for node classification. In *ICLR*, 2020.
- [37] R. J. Sánchez-García. Exploiting symmetry in network analysis. *Communications Physics*, 2020.
- [38] F. Scarselli, M. Gori, A. C. Tsoi, M. Hagenbuchner, and G. Monfardini. The graph neural network model. *IEEE Transactions on Neural Networks*, 20:61–80, 2009.

[39] M. T. Schaub, N. O’Clery, Y. N. Billeh, J.-C. Delvenne, R. Lambiotte, and M. Barahona. Graph partitions and cluster synchronization in networks of oscillators. *Chaos: An Interdisciplinary Journal of Nonlinear Science*, 26(9), 2016.

[40] M. Schlichtkrull, T. Kipf, P. Bloem, R. van den Berg, I. Titov, and M. Welling. Modeling relational data with graph convolutional networks. In *Extended Semantic Web Conference*, 2017.

[41] F. I. Stamm, M. Scholkmper, M. Strohmaier, and M. T. Schaub. Neighborhood structure configuration models. In *WWW*, 2023.

[42] D. Ulyanov, A. Vedaldi, and V. S. Lempitsky. Instance normalization: The missing ingredient for fast stylization. *ArXiv*, abs/1607.08022, 2016.

[43] P. Veličković, G. Cucurull, A. Casanova, A. Romero, P. Liò, and Y. Bengio. Graph attention networks. In *ICLR*, 2018.

[44] B. Weisfeiler and A. Leman. The reduction of a graph to canonical form and the algebra which appears therein. *NTI, Series*, 2(9):12–16, 1968.

[45] S. Wu, W. Zhang, F. Sun, and B. Cui. Graph neural networks in recommender systems: A survey. *ACM Computing Surveys*, 55:1 – 37, 2020.

[46] X. Wu, A. Ajorlou, Z. Wu, and A. Jadbabaie. Demystifying oversmoothing in attention-based graph neural networks. In *NeurIPS*, 2023.

[47] X. Wu, Z. Chen, W. Wang, and A. Jadbabaie. A non-asymptotic analysis of oversmoothing in graph neural networks. In *ICLR*, 2023.

[48] K. Xu, W. Hu, J. Leskovec, and S. Jegelka. How powerful are graph neural networks? In *ICLR*, 2019.

[49] G. Yang, J. Pennington, V. Rao, J. N. Sohl-Dickstein, and S. S. Schoenholz. A mean field theory of batch normalization. In *ICLR*, 2019.

[50] Z. Yang, W. W. Cohen, and R. Salakhutdinov. Revisiting semi-supervised learning with graph embeddings. In *ICML*, 2016.

[51] Y. Yuan, G.-B. Stan, L. Shi, M. Barahona, and J. Goncalves. Decentralised minimum-time consensus. *Automatica*, 2013.

[52] L. Zhao and L. Akoglu. Pairnorm: Tackling oversmoothing in gnns. In *ICLR*, 2020.

[53] K. Zhou, Y. Dong, K. Wang, W. S. Lee, B. Hooi, H. Xu, and J. Feng. Understanding and resolving performance degradation in deep graph convolutional networks. In *CIKM*, 2021.

A Further Background Materials

A.1 An algebraic perspective on the Weisfeiler-Leman coloring

We briefly restate part of what has already been stated in the main text. So that notation is clear again. The Weisfeiler-Leman (WL) algorithm iteratively assigns a color $c(v) \in \mathbb{N}$ to each node $v \in V$ starting from a constant initial coloring $c^{(0)}(v) = 1 \ \forall v \in V$. In each iteration, an update of the following form is computed:

$$c^{(t+1)}(v) = \text{hash} \left(c^{(t)}(v), \{ \{c^{(t)}(x) \mid x \in N(v)\} \} \right) \quad (6)$$

where hash is an injective hash function, and $\{ \cdot \}$ denotes a multiset in which elements can appear more than once. The algorithm returns the final colors $c^{(\infty)}$ when the partition $\{ (c^{(t)})^{-1}(c^{(t)}(v)) \mid v \in V \}$ no longer changes for consecutive t . Morris et al. [34] and Xu et al. [48] showed that GNNs cannot compute different features for nodes that are in the same class in the final coloring $c^{(\infty)}$.

For this paper, the equivalent algebraic perspective of the WL algorithm will be more useful: Given $c^{(\infty)}$ with $\text{Im}(c^{(\infty)}) = \{c_1, \dots, c_k\}$, define $H \in \{0, 1\}^{n \times k}$ such that $H_{v,i} = 1$ if and only if $c^{(\infty)}(v) = c_i$. It holds that

$$AH = H(H^\top H)^{-1}H^\top AH = HA^\pi, \quad (7)$$

where $A^\pi := (H^\top H)^{-1}H^\top AH \in \mathbb{R}^{k \times k}$ is the adjacency matrix of the *quotient graph*. Looking at this equation, there are two things of interest here.

Firstly, $AH = HA^\pi$. Considering this equation more closely, the left side AH counts, for each node, the number of neighbors of color c_i . More formally,

$$(AH)_{v,i} = \sum_{x \in (c^{(\infty)})^{-1}(c_i)} [x \in N(v)] = \sum_{x \in N(v)} [c(x) = c_i]$$

where the Iverson bracket $[\cdot]$ returns 1 if the statement is satisfied and 0 if it is not. The right hand side of the equation (HA^π) states that nodes in the same class have the same rows. It is not hard to verify that if $c^{(\infty)}(v) = c_i$

$$(HA^\pi)_{v,:} = (A^\pi)_{i,:}$$

Now, combining both sides of the equation, the statement $AH = HA^\pi$ reads, that the number of neighbors of any color that a node has is the same for all nodes of the same class meaning $\{ \{c^{(t)}(x) \mid x \in N(v)\} \}$ is the same for all nodes of the class. It becomes clear that at this point we have a fixed point of the WL update equation Equation (6) and conversely whenever we have such a fixed point, the equation $AH = HA^\pi$ holds. The difference between the WL algorithm and Equation (7) is that the latter equation holds for any so called *equitable partition* while the WL algorithm converges to the *coarsest* partition - meaning the partition with fewest distinct colors. For instance, on regular graphs, the WL algorithm returns the partition with 1 color i.e. $H = \mathbb{1}$. However, the trivial partition with n colors $H = I$ also fulfills Equation (7).

Secondly $A^\pi := (H^\top H)^{-1}H^\top AH \in \mathbb{R}^{k \times k}$ is the adjacency matrix of the so-called *quotient graph*. Noticing that $H^\top H = \text{diag}(\{ |(c^{(\infty)})^{-1}(c_i)| \}_{i \in [k]})$ it quickly becomes clear that A^π is the graph of mean connectivity between colors. In other words, a supernode in the quotient graph represent a class of nodes in the original graph who share the same number of neighbors in each final coloring and an edge connecting two such supernodes is weighted by the number of edges there were going from nodes of the one color to nodes of the other color. In this sense, the quotient graph is a compression of the graph structure. It now only has k supernodes compared to the n nodes that there were in the original graph. Still the quotient graph is an adequate depiction of the structure of the graph. Most relevantly, the adjacency matrix A of the original graph inherits all eigenpairs from the quotient graph: Let (λ, ν^π) be an eigenpair of A^π , then

$$AH\nu^\pi = HA^\pi\nu^\pi = \lambda H\nu^\pi.$$

We call such eigenvectors of A the *structural eigenvectors*. They are profoundly important and may even completely determine processes that move over the edges of a network. The structural eigenvectors span a linear subspace that is invariant to multiplication with A . This means that once inside this subspace a graph dynamical system cannot leave it. This holds true for GNNs as Morris et al. [34] and Xu et al. [48] showed.

B Proofs

B.1 Proof for Proposition 4.1

Proposition 4.1. *If $\mu(X^{(0)}) > 0$, then $\mu(X^{(t)}) > 0$ with probability 1.*

Proof. If $\mu(X^{(0)}) > 0$, then, there must be a column in $X^{(0)}$ that is not a scaled version of the all-ones vector - otherwise $\mu(X^{(0)}) = 0$ follows directly. Take this column $X_{:,i}^{(0)} \neq c\mathbb{1}$. Then there exists indices j, l s.t. $X_{j,i}^{(0)} \neq X_{l,i}^{(0)}$. We now prove by induction that with probability 1, $X_{j,i}^{(t)} \neq X_{l,i}^{(t)}$ - which will directly yield the statement.

The base case for the initial features is obviously true.

Consider w.l.o.g the first column in the next iteration:

$$\begin{aligned} X_{:,1}^{(t+1)} &= (1 - \alpha)AX^{(t)}(W_1^{(t)})_{:,1} + \alpha X^{(0)}(W_2^{(t)})_{:,1} \\ &= (1 - \alpha) \sum_{q=1}^k (AX^{(t)})_{:,q}(W_1^{(t)})_{q,1} + \alpha \sum_{q=1}^k X_{:,q}^{(0)}(W_2^{(t)})_{q,1} \\ &= \sum_{q=1}^k (1 - \alpha)(AX^{(t)})_{:,q}(W_1^{(t)})_{q,1} + \alpha X_{:,q}^{(0)}(W_2^{(t)})_{q,1} \end{aligned}$$

Now, looking at the entries j, l , which were distinct for column i in the initial features, we get that:

$$\begin{aligned} X_{j,1}^{(t+1)} &= \sum_{q=1}^k (1 - \alpha)(AX^{(t)})_{j,q}(W_1^{(t)})_{q,1} + \alpha X_{j,q}^{(0)}(W_2^{(t)})_{q,1} \\ &= \sum_{q=1, q \neq i}^k (1 - \alpha)(AX^{(t)})_{j,q}(W_1^{(t)})_{q,1} + \alpha X_{j,q}^{(0)}(W_2^{(t)})_{q,1} \\ &\quad + (1 - \alpha)(AX^{(t)})_{j,i}(W_1^{(t)})_{i,1} + \alpha X_{j,i}^{(0)}(W_2^{(t)})_{i,1} \\ &= \varphi_j^{(t)} + \alpha X_{j,i}^{(0)}(W_2^{(t)})_{i,1} \end{aligned}$$

By the same reasoning, $X_{l,1}^{(t+1)} = \varphi_l^{(t)} + \alpha X_{l,i}^{(0)}(W_2^{(t)})_{i,1}$. Note that both $\varphi_j^{(t)}$ and $\varphi_l^{(t)}$ are not influenced by $(W_2^{(t)})_{i,1}$. To wrap up the proof, we consider the probability that the opposite of what we want to show happens, and show that this has probability 0. Consider:

$$\begin{aligned} \mathcal{A} &= \{W_1^{(t)}, W_2^{(t)} \in \mathbb{R}^{k \times k} \mid X_{j,1}^{(t+1)} = X_{l,1}^{(t+1)}\} \\ &= \{W_1^{(t)}, W_2^{(t)} \in \mathbb{R}^{k \times k} \mid \varphi_j^{(t)} + \alpha X_{j,i}^{(0)}(W_2^{(t)})_{i,1} - \varphi_l^{(t)} - \alpha X_{l,i}^{(0)}(W_2^{(t)})_{i,1} = 0\} \end{aligned}$$

\mathcal{A} defines a proper hyperplane in the space of the randomly sampled weights. As such it has Lebesgue measure 0 - which in turn means it has probability 0. Thus, the probability of the opposite event

$$\mathcal{B} = \{W_1^{(t)}, W_2^{(t)} \in \mathbb{R}^{k \times k} \mid X_{j,i}^{(t)} \neq X_{l,i}^{(t)}\} = \{W_1^{(t)}, W_2^{(t)} \in \mathbb{R}^{k \times k} \mid \mu(X^{(t)}) > 0\}$$

is 1. This concludes the induction and the proof. \square

B.2 Proposition 4.1: deterministic case

For the deterministic version, we adopt the following regularity conditions on weight matrices:

Assumption B.1. For the system described in (4), assume: there exists $\epsilon > 0$ such that

1. $\sum_{m=0}^t \alpha(1 - \alpha)^m \lambda_i^m W_2^{(t-m)} W_1^{(t-m+1)} \cdots W_1^{(t)} + (1 - \alpha)^{t+1} \lambda_i^{t+1} W_1^{(0)} \cdots W_1^{(t)}$ has smallest singular value $\sigma_{\min} \geq \epsilon$ for all $i \in [n]$.
2. $\sum_{m=0}^t \alpha(1 - \alpha)^m \lambda_i^m W_2^{(t-m)} W_1^{(t-m+1)} \cdots W_1^{(t)} + (1 - \alpha)^{t+1} \lambda_i^{t+1} W_1^{(0)} \cdots W_1^{(t)}$ converges as $t \rightarrow \infty$ and has smallest singular value $\sigma_{\min} \geq \epsilon$ for all $i \in [n]$.

Suppose A is full-rank. If weights $W_1^{(t)}, W_2^{(t)}$ are orthogonal, then Assumption B.1.1 holds. On the other hand, Assumption B.1.2 is an asymptotic technical condition to ensure that weights are non-collapsing and non-diverging in the limit. Some ways to satisfy the assumptions is to have the spectral radius of A , $\rho(A) \leq 1$ and $W_1^{(t)}, W_2^{(t)} = I_k$ for any $t \geq 0$.

We restate Proposition 4.1 with full conditions: let $V \in \mathbb{R}^{n \times n}$ be the matrix of eigenvectors for A .

Proposition B.2. *Under Assumption B.1, let $\nu_q \in V$ be such that $\nu_q^\top \mathbf{1} = 0$. If $X^{(0)}$ is properly initialized, such as if $X^{(0)}$ is not the zero matrix and $\|\nu_q^\top X^{(0)}\|_2 = c > 0$, then $\mu(X^{(t)}) \geq c\epsilon/\sqrt{k}$ for all $t \geq 0$ and $\lim_{t \rightarrow \infty} \mu(X^{(t)}) \geq c\epsilon/\sqrt{k}$.*

Proof. Writing (4) recursively, we get that

$$\begin{aligned} X^{(t+1)} &= \alpha \sum_{m=0}^t (1-\alpha)^m A^m X^{(0)} W_2^{(t-m)} W_1^{(t-m+1)} \dots W_1^{(t)} \\ &\quad + (1-\alpha)^{t+1} A^{t+1} X^{(0)} W_1^{(0)} \dots W_1^{(t)}. \end{aligned}$$

For each column $X_{:,i}^{(t+1)}$, similarly, one can prove by induction that

$$X_{:,i}^{(t+1)} = \sum_{l=1}^n \sum_{m=0}^t \sigma_{l,i}^{(t,m)} \lambda_l^m \nu_l,$$

where

- $\Sigma^{(0,0)} = V^\top X^{(0)}$,
- $\Sigma^{(t,0)} = \alpha \Sigma^{(0,0)} W_2^{(t-1)}$ for all $t \geq 0$,
- $\Sigma^{(t,m)} = \alpha(1-\alpha)^m \Sigma^{(0,0)} W_2^{(t-m-1)} W_1^{(t-m)} \dots W_1^{(t-1)}$, for all $1 \leq m \leq t-1$,
- $\Sigma^{(t,t)} = (1-\alpha)^t \Sigma^{(0,0)} W_1^{(0)} \dots W_1^{(t-1)}$.

Then $\nu_q^\top X^{(t)}$

$$= \nu_q^\top X^{(0)} \left(\sum_{m=0}^t \alpha(1-\alpha)^m \lambda_i^m W_2^{(t-m)} W_1^{(t-m+1)} \dots W_1^{(t)} + (1-\alpha)^{t+1} \lambda_i^{t+1} W_1^{(0)} \dots W_1^{(t)} \right). \quad (8)$$

Since by construction, $\|\nu_q^\top X^{(0)}\|_2 = c$, it follows from the regularity conditions on weights that

$$\|\nu_q^\top X^{(t)}\|_2 \geq c\epsilon.$$

This implies that

$$\|\nu_q^\top X^{(t)}\|_\infty \geq c\epsilon/\sqrt{k},$$

which means that there exists $i \in [k]$ such that

$$|\nu_q^\top X_{:,i}^{(t)}| = c\epsilon/\sqrt{k}.$$

Note that since $\nu_q \in V$ and $\nu_q^\top \mathbf{1} = 0$, we get that

$$\begin{aligned} \mu(X^{(t)}) &= \left\| X^{(t)} - \frac{\mathbf{1}\mathbf{1}^\top}{n} X^{(t)} \right\|_F = \sqrt{\sum_{l=1}^k \left\| X_{:,l}^{(t)} - \frac{\mathbf{1}\mathbf{1}^\top}{n} X_{:,l}^{(t)} \right\|_2^2} \\ &\geq \sqrt{\left\| X_{:,i}^{(t)} - \frac{\mathbf{1}\mathbf{1}^\top}{n} X_{:,i}^{(t)} \right\|_2^2} \\ &\geq |\nu_q^\top X_{:,i}^{(t)}| \end{aligned}$$

which means that $\mu(X^{(t)}) \geq c\epsilon/\sqrt{k}$.

Similarly, we can show that $\lim_{t \rightarrow \infty} \mu(X^{(t)}) \geq c\epsilon/\sqrt{k}$. \square

B.3 Proof for Proposition 4.2

Proposition 4.2. Let $x_i = X_{:,i}^{(0)}$ and let $\|x_i\|_2 = 1$ for $i \in [k]$. Let each $(W_l^{(t)})_{y,z} \stackrel{\text{i.i.d.}}{\sim} \mathcal{N}(\eta, s^2)$. Then for any $\epsilon > 0$, $\|x_i^\top X^{(t)}\|_2 \geq \epsilon$ with probability at least $p = 1 - \exp\left(-\frac{\epsilon^2}{2\alpha^2 s^2}\right)$.

Proof. We start by deconstructing $X^{(t)}$ as

$$X^{(t)} = (1 - \alpha)AX^{(t-1)}W_1^{(t-1)} + \alpha X^{(0)}W_2^{(t-1)}$$

This means that:

$$\begin{aligned} x_i^\top X^{(t)} &= (1 - \alpha)x_i^\top AX^{(t-1)}W_1^{(t-1)} + \alpha x_i^\top X^{(0)}W_2^{(t-1)} \\ &= \varphi + \alpha x_i^\top X^{(0)}W_2^{(t-1)} \end{aligned} \tag{9}$$

Resulting in:

$$\begin{aligned} \|x_i^\top X^{(t)}\|_2 &\geq \|x_i^\top X^{(t)}\|_\infty = \|\varphi + \alpha x_i^\top X^{(0)}W_2^{(t-1)}\|_\infty \\ &= \max_j |\varphi_j + \alpha(x_i^\top X^{(0)}W_2^{(t-1)})_j| \\ &\geq |\varphi_j + \alpha(x_i^\top X^{(0)}W_2^{(t-1)})_j| \\ &= |\varphi_j + \alpha x_i^\top (X^{(0)}W_2^{(t-1)})_{:,j}| \\ &= |\varphi_j + \alpha x_i^\top X^{(0)}(W_2^{(t-1)})_{:,j}| \\ &= |\varphi_j + \alpha \sum_a (x_i^\top)_a (X^{(0)})_{a,:} (W_2^{(t-1)})_{:,j}| \\ &= |\varphi_j + \alpha \sum_b \sum_a (x_i^\top)_a (X^{(0)})_{a,b} (W_2^{(t-1)})_{b,j}| = |\hat{Z}| \end{aligned} \tag{10}$$

\hat{Z} is a weighted sum of Gaussian variables and as such, is Gaussian itself ($\mathcal{N}(\hat{\eta}, \hat{s}^2)$) with mean $\hat{\eta} = \eta(\varphi_j) + \eta \sum_b \sum_a (x_i^\top)_a (X^{(0)})_{a,b}$ and variance $\hat{s}^2 = s^2(\varphi_j) + \alpha^2 s^2 \sum_b (\sum_a (x_i^\top)_a (X^{(0)})_{a,b})^2$. Because x_i is normalized, we have that $\sum_a (x_i^\top)_a (X^{(0)})_{a,i} = 1$ and as such $\hat{s}^2 \geq \alpha^2 s^2$.

Define the helper variable \hat{Z}/α , which is Gaussian with $\hat{Z}/\alpha \sim \mathcal{N}(\frac{\hat{\eta}}{\alpha}, \frac{\hat{s}^2}{\alpha^2})$ and define the variable $Z \sim \mathcal{N}(0, s^2)$. Notice that \hat{Z}/α has higher variance than Z . To finish the proof, notice that

$$Pr(|\hat{Z}| \geq \alpha\epsilon) = Pr(|\hat{Z}|/\alpha \geq \epsilon) \geq Pr(|Z| \geq \epsilon) = 1 - Pr(|Z| < \epsilon) \geq 1 - \exp\left(-\frac{\epsilon^2}{2s^2}\right),$$

where the last inequality is based on the Chernoff Bound. \square

B.4 Proposition 4.2: deterministic case

We complement 4.2 with the following result. Let $V \in \mathbb{R}^{n \times n}$ be the matrix of eigenvectors of A and define

$$\begin{aligned} V^* &:= \{\nu_q \in V : \|\nu_q^\top X^{(0)}\|_2 = c_q\} \\ V^0 &:= \{\nu_p \in V : \|\nu_p^\top X^{(0)}\|_2 = 0\}, \end{aligned}$$

where $c_q > 0$ for all q . In words, V^* is the set of eigenspaces of A onto which $X^{(0)}$ has a non-trivial projection, and V^0 is the set of eigenspaces of A onto which $X^{(0)}$ has no projection.

Proposition B.3. Under Assumption B.1.1, for all $t \geq 1$,

$$\|\nu_q^\top X^{(t)}\|_2 = c_q \epsilon, \forall \nu_q \in V^*, \quad \|\nu_p^\top X^{(t)}\|_2 = 0, \forall \nu_p \in V^0.$$

Under Assumption B.1.2,

$$\lim_{t \rightarrow \infty} \|\nu_q^\top X^{(t)}\|_2 > c_q \epsilon, \forall \nu_q \in V^*, \quad \lim_{t \rightarrow \infty} \|\nu_p^\top X^{(t)}\|_2 = 0, \forall \nu_p \in V^0.$$

Proof. The proof follows directly from the form (8). \square

The above result states that the signal excited in the original graph input $X^{(0)}$ is precisely what stays and the signal that is not excited in $X^{(0)}$ can never be created through message-passing.

We give the following concrete example of the above result:

Example Suppose $W_1^{(t)}, W_2^{(t)} = I$, then

$$X^{(t+1)} = \left(\alpha \sum_{k=0}^t (1-\alpha)^k A^k + (1-\alpha)^{t+1} A^{t+1} \right) X.$$

Note that when $\rho(A) < 1/(1-\alpha)$ such as $A = D^{-1/2} A_{\text{adj}} D^{-1/2}$, as $t \rightarrow \infty$,

$$\lim_{t \rightarrow \infty} X^{(t)} = \alpha(I_n - (1-\alpha)A)^{-1} X.$$

Let (λ_i, ν_i) be the i -th eigenpair of A and $\sigma_{l,i} = \langle v_l, X_{:,i} \rangle$, then

$$X_{:,i}^{(t+1)} = \sum_{l=1}^n \left(\sum_{k=1}^t \alpha(1-\alpha)^k \lambda_l^k + (1-\alpha)^{t+1} \lambda_l^{t+1} \right) \sigma_{l,i} \nu_l,$$

and when $\rho(A) < 1/(1-\alpha)$ such as $A = D^{-1/2} A_{\text{adj}} D^{-1/2}$,

$$\lim_{t \rightarrow \infty} X_{:,i}^{(t+1)} = \sum_{l=1}^n \frac{\alpha}{1 - (1-\alpha)\lambda_l} \sigma_{l,i} \nu_l.$$

This implies that for all ν_q ,

$$\begin{aligned} \|\nu_q^\top X^{(t)}\|_2 &= \sqrt{\sum_{i=1}^k \left(\left(\sum_{m=1}^{t-1} \alpha(1-\alpha)^m \lambda_q^m + (1-\alpha)^t \lambda_q^t \right) \sigma_{q,i} \right)^2} \\ &= \left(\sum_{m=1}^{t-1} \alpha(1-\alpha)^m \lambda_q^m + (1-\alpha)^t \lambda_q^t \right) \|\sigma_{q,:}\|_2 \end{aligned}$$

and as $t \rightarrow \infty$,

$$\lim_{t \rightarrow \infty} \|\nu_q^\top X^{(t)}\|_2 = \frac{\alpha}{1 - (1-\alpha)\lambda_q} \|\sigma_{q,:}\|_2.$$

B.5 Proof of Proposition 4.3

Proposition 4.3. Let $\text{Kr}(A, X^{(0)}) = \text{Span}(\{A^{i-1} X_{:,j}^{(0)}\}_{i \in [n], j \in [k]})$ be the Krylov subspace. Let $Y \in \mathbb{R}^{n \times k}$. Then there exist a $T \in \mathbb{N}$ and sequence of weights $W_1^{(0)}, W_2^{(0)}, \dots, W_1^{(T-1)}, W_2^{(T-1)}$ such that $X^{(T)} = Y$ if and only if $Y \in \text{Kr}(A, X^{(0)})$.

Proof. Set $T = n$, $\alpha = 0.5$ and $W_1^{(t)} = I$ for $t > 0$ and $W_1^{(0)} = \emptyset$. Begin by unrolling the recursive equation Equation (4):

$$X^{(1)} = (1-\alpha)AX^{(0)}W_1^{(0)} + \alpha X^{(0)}W_2^{(0)}$$

And in turn:

$$\begin{aligned} X^{(2)} &= (1-\alpha)AX^{(1)}W_1^{(1)} + \alpha X^{(0)}W_2^{(1)} \\ &= (1-\alpha)A((1-\alpha)AX^{(0)}W_1^{(0)} + \alpha X^{(0)}W_2^{(0)})I + \alpha X^{(0)}W_2^{(1)} \\ &= 0.5^2 AX^{(0)}W_2^{(0)} + 0.5 X^{(0)}W_2^{(1)} \end{aligned}$$

Iterating this, yields:

$$X^{(n)} = \sum_{i=1}^n 0.5^i A^{i-1} X^{(0)} W_2^{(i-1)}$$

Now consider a single column of $X^{(n)}$:

$$\begin{aligned} (X^{(n)})_{:,j} &= \sum_{i=1}^n 0.5^i A^{i-1} X^{(0)} (W_2^{(i-1)})_{:,j} \\ &= \sum_{l=1}^k \sum_{i=1}^n 0.5^i (W_2^{(i-1)})_{l,j} A^{i-1} X^{(0)}_{:,l} \end{aligned}$$

Now let $Y_{:,j} \in \text{Kr}(A, X^{(0)})$ be in the Krylov subspace. Then $Y_{:,j} = \sum_{l=1}^k \sum_{i=1}^n w_{l,i} A^{i-1} X^{(0)}_{:,l}$. Setting $(W_2^{(i-1)})_{l,j} = \frac{w_{l,i}}{0.5^i}$ yields $X_{:,j}^{(n)} = Y_{:,j}$.

For the other direction, begin similarly by unrolling the recursive equation:

$$\begin{aligned} X^{(2)} &= (1 - \alpha) A X^{(1)} W_1^{(1)} + \alpha X^{(0)} W_2^{(1)} \\ &= (1 - \alpha) A ((1 - \alpha) A X^{(0)} W_1^{(0)} + \alpha X^{(0)} W_2^{(0)}) W_1^{(1)} + \alpha X^{(0)} W_2^{(1)} \\ &= (1 - \alpha)^2 A^2 X^{(0)} W_1^{(0)} W_1^{(1)} + (1 - \alpha) \alpha A X^{(0)} W_2^{(0)} W_1^{(1)} + \alpha X^{(0)} W_2^{(1)} \end{aligned}$$

Iterating this, yields:

$$X^{(n)} = \sum_{i=1}^{n+1} A^{i-1} X^{(0)} \mathcal{W}^{(i-1)}$$

Now consider a single column of $X^{(n)}$:

$$(X^{(n)})_{:,j} = \sum_{l=1}^k \sum_{i=1}^{n+1} A^{i-1} X^{(0)}_{:,l} \mathcal{W}^{(i-1)}_{l,j}$$

Now, setting $w_{l,i} = \mathcal{W}^{(i-1)}_{l,j}$ and $Y_{:,j} = \sum_{l=1}^k \sum_{i=1}^{n+1} w_{l,i} A^{i-1} X^{(0)}_{:,l}$ verifies that $X_{:,j}^{(n)} = Y_{:,j} \in \text{Kr}(A, X^{(0)})$. \square

B.6 Proof for Proposition 4.5

Proposition 4.5. *Let $\text{Rank}(V_{\neq 0}^\top X^{(0)}) > 1$, then $\mu(X^{(t)}) \geq \sqrt{2}$ for all $t \geq 1$ with probability 1.*

Proof. We prove this by induction. The base case for 0 holds. Assume $\text{Rank}(V_{\neq 0}^\top X^{(t)})$ has rank at least 2. Then, there exist at least 2 columns $X_{:,i}^{(t)}$ and $X_{:,j}^{(t)}$ such that $\text{Rank}(V_{\neq 0}^\top [X_{:,i}^{(t)}, X_{:,j}^{(t)}]) = 2$. Consider their eigenvector decomposition in terms of eigenvectors of $(I - \mathbf{1}\mathbf{1}^\top/n)A$:

$$X_{:,i}^{(t)} = \sum_{l=1}^n \sigma_{l,i}^{(t)} v_l, \quad X_{:,j}^{(t)} = \sum_{l=1}^n \sigma_{l,j}^{(t)} v_l.$$

Consider the action of $(I - \mathbf{1}\mathbf{1}^\top/n)A$:

$$\tilde{X}_{:,i}^{(t)} = (I - \mathbf{1}\mathbf{1}^\top/n) A X_{:,i}^{(t)} = \sum_{l=1}^n \lambda_l \sigma_{l,i}^{(t)} v_l, \quad \tilde{X}_{:,j}^{(t)} = (I - \mathbf{1}\mathbf{1}^\top/n) A X_{:,j}^{(t)} = \sum_{l=1}^n \lambda_l \sigma_{l,j}^{(t)} v_l.$$

Since $X_{:,i}^{(t)}$ and $X_{:,j}^{(t)}$ are linearly independent and the eigenvectors of a symmetric matrix are orthogonal, there exists q such that $\sigma_{q,i}^{(t)} \neq \sigma_{q,j}^{(t)}$ with $\lambda_q \neq 0$. This exists because $\text{Rank}(V_{\neq 0}^\top [X_{:,i}^{(t)}, X_{:,j}^{(t)}]) = 2$. It follows that $\sigma_{q,i}^{(t)} \lambda_q \neq \sigma_{q,j}^{(t)} \lambda_q$, and thus the centered features $\tilde{X}_{:,i}^{(t)} \neq \tilde{X}_{:,j}^{(t)}$ and neither $\tilde{X}_{:,i}^{(t)} = \emptyset$ nor $\tilde{X}_{:,j}^{(t)} = \emptyset$ (otherwise $X_{:,i}^{(t)}$ would be a 0 eigenvector and be orthogonal to $V_{\neq 0}$). Thus, they

are linearly independent. Furthermore, $\tilde{X}_{:,i}^{(t)}, \tilde{X}_{:,j}^{(t)}, \mathbf{1}$ are linearly independent, since $(I - \mathbf{1}\mathbf{1}^\top/n)$ projects to the space orthogonal to $\text{Span}\{\mathbf{1}\}$. Write:

$$\begin{aligned} X_{:,i}^{(t+1)} &= \frac{1}{\Gamma_i} (I - \mathbf{1}\mathbf{1}^\top/n) A X^{(t)} W_{:,i}^{(t)} \\ &= \frac{1}{\Gamma_i} \sum_{a=1}^k W_{a,i}^{(t)} \tilde{X}_{:,a}^{(t)} \\ &= \frac{1}{\Gamma_i} \sum_{a=1, a \neq i, a \neq j}^k W_{a,i}^{(t)} \tilde{X}_{:,a}^{(t)} + W_{i,i}^{(t)} \tilde{X}_{:,i}^{(t)} + W_{j,i}^{(t)} \tilde{X}_{:,j}^{(t)} \\ &= \frac{1}{\Gamma_i} (\varphi^{(i)} + W_{i,i}^{(t)} \tilde{X}_{:,i}^{(t)} + W_{j,i}^{(t)} \tilde{X}_{:,j}^{(t)}). \end{aligned}$$

We now consider the event that column i collapses to the all-ones space. Notice that dividing the whole column by Γ_i does not change whether or not the column has converged to the all-ones space or not. Thus,

$$\begin{aligned} \mathcal{A} &= \{W^{(t)} \in \mathbb{R}^{k \times k} \mid X_{:,i}^{(t+1)} = \beta \mathbf{1}\} \\ &= \{W^{(t)} \in \mathbb{R}^{k \times k} \mid \frac{1}{\Gamma_i} (\varphi^{(i)} + W_{i,i}^{(t)} \tilde{X}_{:,i}^{(t)} + W_{j,i}^{(t)} \tilde{X}_{:,j}^{(t)}) = \beta \mathbf{1}\} \\ &= \{W^{(t)} \in \mathbb{R}^{k \times k} \mid \varphi^{(i)} + W_{i,i}^{(t)} \tilde{X}_{:,i}^{(t)} + W_{j,i}^{(t)} \tilde{X}_{:,j}^{(t)} = \beta' \mathbf{1}\} \\ &= \{W^{(t)} \in \mathbb{R}^{k \times k} \mid W_{i,i}^{(t)} \tilde{X}_{:,i}^{(t)} + W_{j,i}^{(t)} \tilde{X}_{:,j}^{(t)} - \beta' \mathbf{1} = -\varphi^{(i)}\} \end{aligned}$$

Since $\tilde{X}_{:,i}^{(t)}, \tilde{X}_{:,j}^{(t)}, \mathbf{1}$ are linearly independent, given $\varphi^{(i)}$, there is only 1 solution to this equation. \mathcal{A} is a proper hyperplane in $\mathbb{R}^{k \times k}$ and as such has Lebesgue measure 0. The event \mathcal{A} thus has probability 0 and the opposite event, that column i does not collapse to the all-ones space, has probability 1.

The same holds for $X_{:,j}^{(t+1)}$ and by the same reasoning, $X_{:,i}^{(t+1)}$ and $X_{:,j}^{(t+1)}$ are linearly independent with probability 1. Notice, that thus $\text{Rank}(V_{\neq 0}^\top [X_{:,i}^{(t+1)}, X_{:,j}^{(t+1)}]) = 2$ still holds. Finally, because both $\tilde{X}_{:,i}^{(t)}$ and $\tilde{X}_{:,j}^{(t)}$ have variance greater than 0 and the rescaling will make it so that they have variance exactly 1. This means, that $X_{:,i}^{(t+1)}, X_{:,j}^{(t+1)}$ has norm 1 and all columns are centered. We conclude that with probability 1,

$$\mu(X^{(t+1)}) := \left\| X^{(t+1)} - \mathbf{1}\mathbf{1}^\top X^{(t+1)}/n \right\|_F = \left\| X^{(t+1)} \right\|_F \geq \sqrt{2}.$$

□

B.7 Proposition 4.5: general conditions

We adopt the following regularity conditions:

Assumption B.4. For the system described in (5), assume:

1. For nonzero $x \in \mathbb{R}^n$ such that $x^\top \mathbf{1} = 0$, $Ax \notin \text{Span}\{\mathbf{1}\}$.
2. If $\mu((AX^{(t)})_{:,i}) > 0$, then $\mu((AX^{(t)}W^{(t)})_{:,i}) > 0$ for all $i \in [k]$.

Assumption B.4.1 ensure that the adversarial situation where one step of message-passing automatically leads to oversmoothing does not happen. Note that this is a more relaxed condition than requiring $\text{Span}\{\mathbf{1}\}^\perp$ to be an invariant subspace of A .

Assumption B.4.2 ensures that the case where weights are deliberately chosen for oversmoothing to happen in one layer does not happen, either. Note that for the second condition, such weights exist, i.e. let $W^{(t)} = I_k$. Moreover, if weights are randomly initialized, then Assumption B.4.2 holds almost surely.

We restate Proposition 4.5 under general conditions, which accounts for both linear and non-linear systems:

Proposition B.5. For the system in (5), suppose $\sigma(\cdot)$ is injective and Assumption B.4 holds. Without loss of generality, also suppose the initial features $X^{(0)}$ are centered and all columns are nonzero. If $\mu(X^{(0)}) > 0$, then $\mu(X^{(t)}) = \sqrt{k}$ for all $t \geq 1$.

Proof. For each column in $X^{(0)}$, since it is centered and nonzero, $X_{:,i}^{(0)} \in \text{Span}\{\mathbf{1}\}^\perp \setminus \{\mathbf{0}\}$ for all $i \in [k]$.

Then given Assumption B.4.1, $AX_{:,i}^{(0)} \notin \text{Span}\{\mathbf{1}\}$ and thus can be written as

$$AX_{:,i}^{(0)} = a\mathbf{1} + w_0^\perp,$$

where $a \in \mathbb{R}$, $w_0^\perp \in \text{Span}\{\mathbf{1}\}^\perp$ and $w_0^\perp \neq \mathbf{0}$.

Then given Assumption B.4.2, $AX^{(0)}W_{:,i}^{(0)} \notin \text{Span}\{\mathbf{1}\}$ and since $\sigma(\cdot)$ is injective, $\sigma(AX^{(0)}W_{:,i}^{(0)}) \notin \text{Span}\{\mathbf{1}\}$ and

$$\sigma(AX^{(0)}W_{:,i}^{(0)}) = b\mathbf{1} + w_1^\perp,$$

where $b \in \mathbb{R}$, $w_1^\perp \in \text{Span}\{\mathbf{1}\}^\perp$ and $w_1^\perp \neq \mathbf{0}$.

Then after the centering step of batch normalization,

$$(I - \mathbf{1}\mathbf{1}^\top/n)\sigma(AX^{(0)}W_{:,i}^{(0)}) = w_1^\perp,$$

and after the scaling step of batch normalization,

$$X_{:,i}^{(1)} = \text{BN}(\sigma(AX^{(0)}W_{:,i}^{(0)})) = \frac{w_1^\perp}{\|w_1^\perp\|_2},$$

which means each column of $X^{(1)} \in \text{Span}\{\mathbf{1}\}^\perp \setminus \{\mathbf{0}\}$ and has norm 1. This directly implies $\mu(X^{(1)}) = \sqrt{k}$.

The above argument applies for all $t \geq 0$ going from $X^{(t)}$ to $X^{(t+1)}$, which concludes the proof. \square

B.8 If nonlinearity $\sigma(\cdot)$ is applied after batch normalization

Suppose the GNN with batch normalization defined in (5) is instead

$$X^{(t+1)} = \sigma(Y^{(t+1)}), \quad Y^{(t+1)} = \text{BN}(AX^{(t)}W^{(t)}). \quad (11)$$

Suppose $\mathbf{1}$ is an eigenvector of A . Then without $\text{BN}(\cdot)$, [36] showed that $\mu(X^{(t)})$ under appropriate assumptions on the weight matrices. We show the following claim for $X^{(0)}$ where $\mu(X_{:,i}^{(0)}) > 0$:

Proposition B.6. Suppose $\mathbf{1}$ is an eigenvector of A . If $\sigma(\cdot)$ is injective, then under Assumption B.4.2, $\mu(X_{:,i}^{(t)}) > 0$ for all $t \geq 1$ and $i \in [k]$.

Proof. Given $\mu(X_{:,i}^{(0)}) > 0$, $X_{:,i}^{(0)} \notin \text{Span}\{\mathbf{1}\}$ and hence

$$X_{:,i}^{(0)} = a\mathbf{1} + w_0^\perp,$$

where $a \in \mathbb{R}$, $w_0^\perp \in \text{Span}\{\mathbf{1}\}^\perp$ and $w_0^\perp \neq \mathbf{0}$.

Since $\mathbf{1}$ is an eigenvector of A ,

$$AX_{:,i}^{(0)} = b\mathbf{1} + w_1^\perp,$$

where $b \in \mathbb{R}$, $w_1^\perp \in \text{Span}\{\mathbf{1}\}^\perp$ and $w_1^\perp \neq \mathbf{0}$, meaning that $AX_{:,i}^{(0)} \notin \text{Span}\{\mathbf{1}\}$. Then given Assumption B.4.2, $AX^{(0)}W_{:,i}^{(0)} \notin \text{Span}\{\mathbf{1}\}$ and

$$AX^{(0)}W_{:,i}^{(0)} = c\mathbf{1} + w_2^\perp,$$

where $c \in \mathbb{R}$, $w_2^\perp \in \text{Span}\{\mathbf{1}\}^\perp$ and $w_2^\perp \neq \mathbf{0}$.

Then after the centering step of batch normalization,

$$(I - \mathbf{1}\mathbf{1}^\top/n)AX^{(0)}W_{:,i}^{(0)} = w_2^\perp,$$

and after the scaling step of batch normalization,

$$Y_{:,i}^{(1)} = \text{BN}(AX^{(0)}W_{:,i}^{(0)}) = \frac{w_2^\perp}{\|w_2^\perp\|_2},$$

which means each column of $Y^{(1)} \in \text{Span}\{\mathbf{1}\}^\perp \setminus \{\mathbf{0}\}$ and has norm 1.

Then since $\sigma(\cdot)$ is injective, it follows that $X_{:,i}^{(1)} = \sigma(Y_{:,i}^{(1)}) \notin \text{Span}\{\mathbf{1}\}$ and we conclude that $\mu(X_{:,i}^{(1)}) > 0$.

Note that the above argument applies for all $t \geq 0$ going from $X^{(t)}$ to $X^{(t+1)}$, which concludes the proof. \square

B.9 Proof for Proposition 4.7

Proposition 4.7. Suppose $V_k^\top X^{(0)}$ has rank k , then for all weights $W^{(t)}$, the GNN with BatchNorm given in (5) exponentially converges to the column space of V_k .

Proof. We will prove by induction on t that

$$X_{:,i}^{(t)} = \frac{1}{\Gamma^{(t)}} \sum_{l=1}^n \sigma_{l,i}^{(t)} \lambda_l^t \nu_l \quad (12)$$

where (λ_i, ν_i) is the i -th eigenpair of $(I_n - \mathbf{1}\mathbf{1}^\top/n)A$ with $|\lambda_1| \geq |\lambda_2| \geq \dots \geq |\lambda_n|$, $\Gamma^{(t)}$ is the normalization factor in the t -th round and $\sigma_{l,i}^{(t)} \in \mathbb{R}$. The base case follows from the decomposition of $X^{(0)}$ in the eigenvector basis of $(I_n - \mathbf{1}\mathbf{1}^\top/n)A$: $X_{:,i}^{(0)} = \sum_{l=1}^n \langle X_{:,i}^{(0)}, \nu_l \rangle \nu_l$ (and the fact that $X^{(0)}$ is normalized).

For the induction step, the system can be rewritten as

$$\begin{aligned} X^{(t+1)} &= (AX^{(t)}W^{(t)} - \mathbf{1}\mathbf{1}^\top AX^{(t)}W^{(t)}/n) \text{diag}(\dots, \frac{1}{\text{var}((AX^{(t)}W^{(t)})_{:,i})}, \dots) \\ &= (I_n - \mathbf{1}\mathbf{1}^\top/n)AX^{(t)}W^{(t)}D_{\text{var}}. \end{aligned}$$

Assuming Equation (12),

$$((I_n - \mathbf{1}\mathbf{1}^\top/n)AX^{(t)})_{:,i} = \frac{1}{\Gamma^{(t)}} \sum_{l=1}^n \sigma_{l,i}^{(t)} \lambda_l^{t+1} \nu_l.$$

Further the action of $W^{(t)}$ is the following:

$$\begin{aligned} ((I_n - \mathbf{1}\mathbf{1}^\top/n)AX^{(t)}W^{(t)})_{:,i} &= \frac{1}{\Gamma^{(t)}} \sum_{j=1}^k W_{j,i}^{(t)} \sum_{l=1}^n \sigma_{l,j}^{(t)} \lambda_l^{t+1} \nu_l \\ &= \frac{1}{\Gamma^{(t)}} \sum_{l=1}^n \sum_{j=1}^k (W_{j,i}^{(t)} \sigma_{l,j}^{(t)}) \lambda_l^{t+1} \nu_l \\ &= \frac{1}{\Gamma^{(t)}} \sum_{l=1}^n \sigma_{l,i}^{(t+1)} \lambda_l^{t+1} \nu_l. \end{aligned} \quad (13)$$

Notice that $\sigma_{l,i}^{(t+1)} = \sum_{j=1}^k (W_{j,i}^{(t)} \sigma_{l,j}^{(t)})$ or equivalently, $\Sigma^{(t+1)} = \Sigma^{(t)} W^{(t)}$, where $\Sigma^{(t)} = [\sigma_{l,i}^{(t)}]$. Thus, $\Sigma^{(t+1)} = \Sigma^{(0)} W^{(0)} W^{(1)} \dots W^{(t)}$. Lastly, the action of D_{var} is:

$$\begin{aligned}
((I_n - \mathbf{1}\mathbf{1}^\top/n) A X^{(t)} W^{(t)} D_{\text{var}})_{:,i} &= \frac{1}{\|\frac{1}{\Gamma^{(t)}} \sum_{l=1}^n \sigma_{l,i}^{(t+1)} \lambda_l^{t+1} \nu_l\|_2} \frac{1}{\Gamma^{(t)}} \sum_{l=1}^n \sigma_{l,i}^{(t+1)} \lambda_l^{t+1} \nu_l \\
&= \frac{1}{\left| \frac{1}{\Gamma^{(t)}} \sqrt{\sum_{l=1}^n (\sigma_{l,i}^{(t+1)} \lambda_l^{t+1})^2} \right|} \frac{1}{\Gamma^{(t)}} \sum_{l=1}^n \sigma_{l,i}^{(t+1)} \lambda_l^{t+1} \nu_l \\
&= \frac{1}{\left| \sqrt{\sum_{l=1}^n (\sigma_{l,i}^{(t+1)} \lambda_l^{t+1})^2} \right|} \sum_{l=1}^n \sigma_{l,i}^{(t+1)} \lambda_l^{t+1} \nu_l \\
&= \frac{1}{\Gamma^{(t+1)}} \sum_{l=1}^n \sigma_{l,i}^{(t+1)} \lambda_l^{t+1} \nu_l.
\end{aligned}$$

This concludes the induction. Notice that superscripts in brackets do not denote exponentiation, but rather an iterate at iteration t . Using this intermediate result (12), we show the following:

Lemma B.7. *For all $q > k$,*

$$\|\nu_q^\top X^{(t)}\|_2 \leq C_0 \left(\frac{\lambda_q}{\lambda_k} \right)^t.$$

Proving this directly yields Proposition 4.7. We have that $\Sigma^{(0)} = V^\top X^{(0)}$ due to the base case of the induction and by assumption, $\Sigma_{:k,:}^{(0)} = V_k^\top X^{(0)} \in \mathbb{R}^{k \times k}$ has rank k and is therefore full rank. It is therefore invertible, meaning that there exists $(\Sigma_{:k,:}^{(0)})^{-1} \in \mathbb{R}^{k \times k}$ such that $V_k^\top X^{(0)} (\Sigma_{:k,:}^{(0)})^{-1} = I_k$.

We can thus write for the simplicity of notation:

$$\Sigma^{(0)} = \Sigma^{(0)} (\Sigma_{:k,:}^{(0)})^{-1} \Sigma_{:k,:}^{(0)} = \Sigma^{(\perp)} W^{(\perp)} = \begin{bmatrix} I_k \\ \Sigma_{(k+1),:,:}^{(\perp)} \end{bmatrix} W^{(\perp)}.$$

This has the nice property that $\sigma_{i,i}^{(\perp)} = 1$ for $i \leq k$. Now, let's revisit Equation (13) in that we can write $\Sigma^{(t+1)} = \Sigma^{(0)} W^{(0)} W^{(1)} \dots W^{(t)}$. Let $\mathcal{W}^{(t)} = W^{(\perp)} W^{(0)} \dots W^{(t)}$, meaning that $\sigma_{i,j}^{(t)} = \sum_{l=1}^k \mathcal{W}_{i,l}^{(t)} \sigma_{l,j}^{(\perp)}$. We now have everything to conclude the proof:

Consider now, the contribution of an eigenvector ν_q with $q > k$ at iteration t .

$$\begin{aligned}
\|\nu_q^\top X^{(t)}\|_2 &= \sqrt{\sum_{i=1}^k (\nu_q^\top X_{:,i}^{(t)})^2} = \sqrt{\sum_{i=1}^k \left(\frac{1}{\Gamma_i^{(t)}} \sum_{l=1}^n \sigma_{l,i}^{(t)} \lambda_l^{t+1} \nu_l^\top \nu_l \right)^2} = \sqrt{\sum_{i=1}^k \left(\frac{1}{\Gamma_i^{(t)}} \sigma_{q,i}^{(t)} \lambda_q^{t+1} \right)^2} \\
&= \sqrt{\sum_{i=1}^k \frac{(\sigma_{q,i}^{(t)} \lambda_q^{t+1})^2}{\sum_{p=0}^n (\sigma_{p,i}^{(t)} \lambda_p^{t+1})^2}} = \sqrt{\sum_{i=1}^k \frac{(\sum_{l=1}^k \mathcal{W}_{l,i}^{(t)} \sigma_{q,l}^{(\perp)} \lambda_q^{t+1})^2}{\sum_{p=1}^n (\sum_{l=1}^k \mathcal{W}_{l,i}^{(t)} \sigma_{p,l}^{(\perp)} \lambda_p^{t+1})^2}} \\
&\leq \sqrt{\sum_{i=1}^k \frac{(\sum_{l=1}^k \mathcal{W}_{l,i}^{(t)} \sigma_{q,l}^{(\perp)} \lambda_q^{t+1})^2}{\sum_{p=1}^k (\mathcal{W}_{p,i}^{(t)} \sigma_{p,p}^{(\perp)} \lambda_p^{t+1})^2}} = \sqrt{\sum_{i=1}^k \frac{(\sum_{l=1}^k \mathcal{W}_{l,i}^{(t)} \sigma_{q,l}^{(\perp)} \lambda_q^{t+1})^2}{\sum_{p=1}^k (\mathcal{W}_{p,i}^{(t)} \lambda_p^{t+1})^2}} \\
&\leq \sqrt{\sum_{l=1}^k (\sigma_{q,l}^{(\perp)})^2 \sum_{i=1}^k \frac{\sum_{l=1}^k (\mathcal{W}_{l,i}^{(t)} \lambda_q^{t+1})^2}{\sum_{p=1}^k (\mathcal{W}_{p,i}^{(t)} \lambda_p^{t+1})^2}} \\
&\leq \sqrt{\sum_{l=1}^k (\sigma_{q,l}^{(\perp)})^2 \sum_{i=1}^k \frac{\sum_{l=1}^k (\mathcal{W}_{l,i}^{(t)} \lambda_q^{t+1})^2}{\sum_{p=1}^k (\mathcal{W}_{p,i}^{(t)} \lambda_p^{t+1})^2}} = \sqrt{\sum_{l=1}^k (\sigma_{q,l}^{(\perp)})^2 k \frac{\lambda_q^{t+1}}{\lambda_k^{t+1}}} \\
&\leq C_0 \frac{\lambda_q^{t+1}}{\lambda_k^{t+1}}.
\end{aligned}$$

As we have that $\lambda_q < \lambda_k$ by construction, $\|\nu_q^\top X^{(t)}\|_2 \rightarrow 0$ exponentially as $t \rightarrow \infty$. \square

B.10 Proof for Proposition 4.8

Proposition 4.8. Suppose $|\hat{\lambda}_k| > 0$ and $V_k^\top X^{(0)}$ has rank k . For any $\epsilon > 0$, there exists $T > 0$ and a sequence of weights $W^{(0)}, W^{(1)}, \dots, W^{(T)}$ such that for all $t \geq T$ and $i \in [k]$,

$$\left\| \nu_i^\top X_{:,i}^{(t)} \right\|_2 \geq 1/\sqrt{1+\epsilon},$$

where ν_i denotes the i -th eigenvector of $(I_n - \mathbf{1}\mathbf{1}^\top/n)A$.

Proof. The proof idea is simple: we use Gaussian elimination to cancel out all “top-k” eigenvectors but the one in that row and then use the power iteration until the smaller eigenvectors are “drowned out” below the ϵ error margin. Assuming the columns of $X_{:,k+1}^{(0)}$ are linearly independent (which is the case if it has rank k), this leads to the desired output: choose

$$W_{j,i}^{(0)} = \begin{cases} 1 & \text{if } j = i \\ -\frac{\sigma_{1,i}^{(0)}}{\sigma_{1,1}^{(0)}} & \text{if } j = 1 \text{ and } i \neq 1 \\ 0 & \text{else} \end{cases}$$

Then from Equation (13) for each column $X_{:,i}$, we get that

$$X_{:,i}^{(1)} = \frac{1}{\Gamma_i^{(1)}} \sum_{l=1}^n \sum_{j=1}^k (W_{j,i}^{(0)} \sigma_{l,j}^{(0)}) \lambda_l^1 \nu_l = \frac{1}{\Gamma_i^{(1)}} \sum_{l=1}^n (\sigma_{l,i}^{(0)} - \frac{\sigma_{1,i}^{(0)}}{\sigma_{1,1}^{(0)}} \sigma_{l,1}^{(0)}) \lambda_l^1 \nu_l.$$

Now for $l = 1$, the factor $\sigma_{l,i}^{(0)} - \frac{\sigma_{1,i}^{(0)}}{\sigma_{1,1}^{(0)}} \sigma_{l,1}^{(0)} = 0$ yields

$$X_{:,i}^{(1)} = \frac{1}{\Gamma_i^{(1)}} \sum_{l=2}^n (\sigma_{l,i}^{(0)} - \frac{\sigma_{1,i}^{(0)}}{\sigma_{1,1}^{(0)}} \sigma_{l,1}^{(0)}) \lambda_l^1.$$

Iterating this idea and choosing

$$W_{j,i}^{(k)} = \begin{cases} 1 & \text{if } j = i \\ -\frac{\sigma_{k+1,i}^{(k)}}{\sigma_{k+1,k+1}^{(k)}} & \text{if } j = k+1 \text{ and } i \neq k+1 \\ 0 & \text{else,} \end{cases}$$

we arrive at

$$X_{:,i}^{(k)} = \frac{1}{\Gamma_i^{(k)}} \left(\sigma_{i,i}^{(i-1)} \lambda_i^k \nu_i + \sum_{l=k+1}^n \sigma_{l,i}^{(k)} \lambda_l^k \nu_l \right).$$

Now, we switch gears and use $W^{(t)} = I_n$ for $t \geq k$, it follows that

$$\begin{aligned} \|\nu_i^\top (X_{:,i}^{(t)})\|_2 &= \frac{\sigma_{i,i}^{(i-1)} \lambda_i^t}{\sqrt{(\sigma_{i,i}^{(i-1)} \lambda_i^t)^2 + \sum_{l=k+1}^n (\sigma_{l,i}^{(k)} \lambda_l^t)^2}} \\ &= \frac{1}{\sqrt{1 + \frac{\sum_{l=k+1}^n (\sigma_{l,i}^{(k)} \lambda_l^t)^2}{(\sigma_{i,i}^{(i-1)} \lambda_i^t)^2}}}. \end{aligned}$$

The statement left to prove is thus:

$$\begin{aligned}
\epsilon &\geq \frac{\sum_{l=k+1}^n (\sigma_{l,i}^{(k)} \lambda_l^t)^2}{(\sigma_{i,i}^{(i-1)} \lambda_i^t)^2} \\
\iff \epsilon &\geq \frac{(n-k) \max_l (\sigma_{l,i}^{(k)})^2}{(\sigma_{i,i}^{(i-1)})^2} \frac{\lambda_{k+1}^{2t}}{\lambda_i^{2t}} \\
\iff \frac{\log \left(\frac{\epsilon \sigma_{i,i}^{(i-1)}}{(n-k) \max_l (\sigma_{l,i}^{(k)})^2} \right)}{2 \log \left(\frac{\lambda_{k+1}}{\lambda_i} \right)} &\leq t.
\end{aligned}$$

Thus, setting T to be larger than this bound yields the desired claim. \square

B.11 Proof for Proposition 5.1

Proposition B.8. *Let $A \in \mathbb{R}_{\geq 0}^{n \times n}$ be a symmetric non-negative matrix. Let $H \in \{0, 1\}^{n \times m}$ such that $AH = HA^\pi$ is the coarsest EP of A . Divide the eigenpairs $\mathcal{V} = \{..., (\lambda, \nu), ...\}$ of A into the following two sets: $\mathcal{V}_{\text{struc}} = \{(\lambda, \nu) \in \mathcal{V} \mid \nu = H\nu^\pi\}$, $\mathcal{V}_{\text{rest}} = \mathcal{V} \setminus \mathcal{V}_{\text{struc}}$. Let $\hat{\mathcal{V}} = \{..., (\hat{\lambda}, \hat{\nu}), ...\}$ be eigenpairs of $(I_n - \tau \mathbf{1}\mathbf{1}^\top/n)A$, for $\tau \neq 0$. Then*

1. $\mathcal{V}_{\text{rest}} \subset \hat{\mathcal{V}}$.
2. Assume $\mathcal{V}_{\text{struc}} \neq \{(\lambda, \mathbf{1})\}$. Let (λ, ν) be the dominant eigenpair of A . Then ν is **not** an eigenvector of $(I_n - \tau \mathbf{1}\mathbf{1}^\top/n)A$.
3. $\sum_{(\lambda, \nu) \in \mathcal{V}_{\text{struc}}} \lambda > \sum_{(\hat{\lambda}, \hat{\nu}) \in \hat{\mathcal{V}} \setminus \mathcal{V}_{\text{rest}}} \hat{\lambda}$

Proof. Let $H \in \{0, 1\}^{n \times m}$ indicate the coarsest EP of A ($AH = HA^\pi$). As each node belongs to exactly 1 class, it holds that $H\mathbf{1}_n = \mathbf{1}_m$. We prove that for any eigenpair $(\lambda, \nu) \in \mathcal{V}_{\text{rest}}$, it holds that $\nu^\top \mathbf{1} = 0$. From this, the first statement follows quickly:

$$(I_n - \tau \mathbf{1}\mathbf{1}^\top/n)A\nu = A\nu - \tau \mathbf{1}\mathbf{1}^\top A\nu/n = \lambda\nu - \tau \lambda \mathbf{1}\mathbf{1}^\top \nu/n = \lambda\nu.$$

To prove this, let's look at A^π . A^π is not symmetric, but its eigenpairs are associated to A 's eigenpairs in the following way. Let (λ, ν^π) be an eigenpair of A^π , then $(\lambda, H\nu^\pi)$ is an eigenpair of A : $AH\nu^\pi = HA^\pi = H\lambda\nu^\pi$. As A is a symmetric matrix, its eigenvectors are orthogonal implying $(H\nu_i^\pi)^\top (H\nu_j^\pi) = 0$.

Lemma B.9. *The eigenvectors $\nu_1^\pi, \dots, \nu_m^\pi$ of A^π are linearly independent.*

For simplicity, choose the eigenvectors ν_i^π to be normalized in such a way, that $(H\nu_i^\pi)^\top (H\nu_i^\pi) = 1$. Suppose for a contradiction, that they are linearly dependent and without loss of generality, $\nu_m^\pi = \sum_{i=1}^{m-1} a_i \nu_i^\pi$. Take j such that $a_j \neq 0$, this must exist otherwise $\nu_m = \mathbf{0}$. Now,

$$(H\nu_m^\pi)^\top (H\nu_j^\pi) = (H \sum_{i=1}^{m-1} a_i \nu_i^\pi)^\top (H\nu_j^\pi) = \sum_{i=1}^{m-1} (Ha_i \nu_i^\pi)^\top (H\nu_j^\pi) = a_j \neq 0,$$

which is a contradiction.

Since the eigenvectors of A^π are linearly independent, there exists a unique $\beta \in \mathbb{R}^m$ s.t. $\sum_{i=1}^m \beta_i \nu_i^\pi = \mathbf{1}_m$. Finally let $\varphi \in \mathcal{V}_{\text{rest}}$,

$$\varphi^\top \mathbf{1}_n = \varphi^\top H\mathbf{1}_m = \varphi^\top H \sum_{i=1}^m \beta_i \nu_i^\pi = \sum_{i=1}^m \beta_i \varphi^\top H \nu_i^\pi = 0.$$

This concludes the proof of the first statement.

To prove the second statement, let (λ, ν) be a dominant eigenpair of A , such that $\nu \geq 0$ is non-negative. This exists as A is a non-negative matrix. Additionally, ν is not the all-zeros vector and as such $\mathbf{1}^\top \nu > 0$. By assumption $\nu \neq \mathbf{1}$. Then:

$$(I - \tau \mathbf{1} \mathbf{1}^\top / n) A \nu = \hat{\lambda} \nu \iff \lambda \nu - \tau \mathbf{1} \mathbf{1}^\top \lambda \nu / n = \hat{\lambda} \nu \iff (\lambda - \hat{\lambda}) \nu - \tau \lambda \mathbf{1} \mathbf{1}^\top \nu / n = 0.$$

As $\nu \neq \mathbf{1}$, there exist i, j s.t. $\nu_i \neq \nu_j$ thus, $(\lambda - \hat{\lambda}) \nu_i - \tau \lambda (\mathbf{1} \mathbf{1}^\top \nu)_i / n = 0$ and $(\lambda - \hat{\lambda}) \nu_j - \tau \lambda (\mathbf{1} \mathbf{1}^\top \nu)_j / n = 0$ cannot be true at the same time. Thus, this equation has no solution and ν is not an eigenvector of $(I_n - \tau \mathbf{1} \mathbf{1}^\top / n) A$.

For the third and final statement, notice that the trace of A is larger than the trace of $(I_n - \tau \mathbf{1} \mathbf{1}^\top / n) A$. Since the trace of a matrix is the sum of its eigenvalues, we have

$$\sum_{(\lambda, \nu) \in \mathcal{V}} \lambda = \text{Tr}(A) > \text{Tr}((I_n - \tau \mathbf{1} \mathbf{1}^\top / n) A) = \sum_{(\hat{\lambda}, \hat{\nu}) \in \hat{\mathcal{V}}} \hat{\lambda}.$$

Consequently,

$$\sum_{(\lambda, \nu) \in \mathcal{V}} \lambda = \sum_{(\lambda, \nu) \in \mathcal{V}_{\text{struc}}} \lambda + \sum_{(\lambda, \nu) \in \mathcal{V}_{\text{rest}}} \lambda > \sum_{(\hat{\lambda}, \hat{\nu}) \in \hat{\mathcal{V}} \setminus \mathcal{V}_{\text{rest}}} \hat{\lambda} + \sum_{(\lambda, \nu) \in \mathcal{V}_{\text{rest}}} \lambda = \sum_{(\hat{\lambda}, \hat{\nu}) \in \hat{\mathcal{V}}} \hat{\lambda}.$$

Subtracting $\sum_{(\lambda, \nu) \in \mathcal{V}_{\text{rest}}} \lambda$ from both sides yields the final statement.

□

C Experiments

We compare these models using the measures of convergence: $\mu(X^{(t)})$ as defined in (3), the numerical rank of the features $\text{Rank}(X^{(t)})$, the column distance used in [52]:

$$d_{\text{col}}(X) := \frac{1}{d^2} \sum_{i,j} \left\| \frac{X_{:,i}}{\|X_{:,i}\|_1} - \frac{X_{:,j}}{\|X_{:,j}\|_1} \right\|_2,$$

the column projection distance:

$$d_{\text{p-col}}(X) := \frac{1}{d^2} \sum_{i,j} 1 - \frac{X_{:,i}^\top}{\|X_{:,i}\|_2} \frac{X_{:,j}}{\|X_{:,j}\|_2},$$

and the eigenvector space projection:

$$d_{\text{ev}}(X) := \frac{1}{n} \|X - VV^\top X\|_F,$$

where $V \in \mathbb{R}^{n \times n}$ is the set of normalized eigenvectors of A , and finally, the rank of X : $\text{Rank}(X)$. The same experiment with both GIN and GAT can be found below. The trends are similar to those described in the main manuscript.

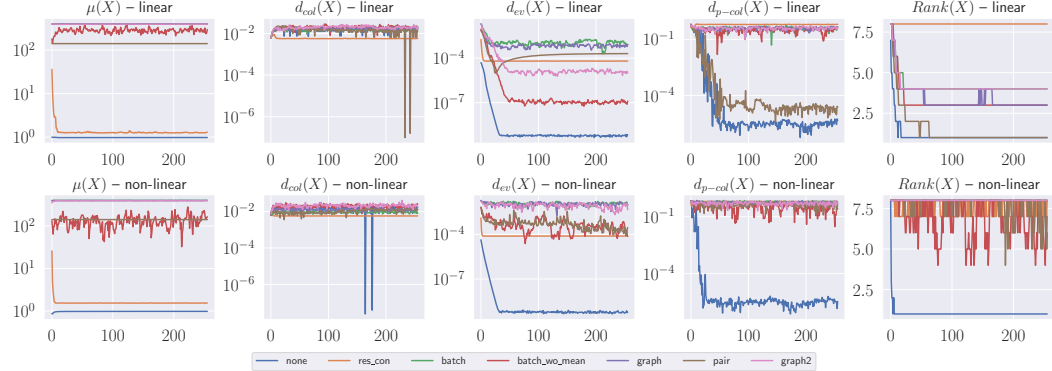


Figure 2: Long Term behavior of GCN. Progression of the above measures of convergence over 256 iterations of message-passing in both linear and non-linear GCN.

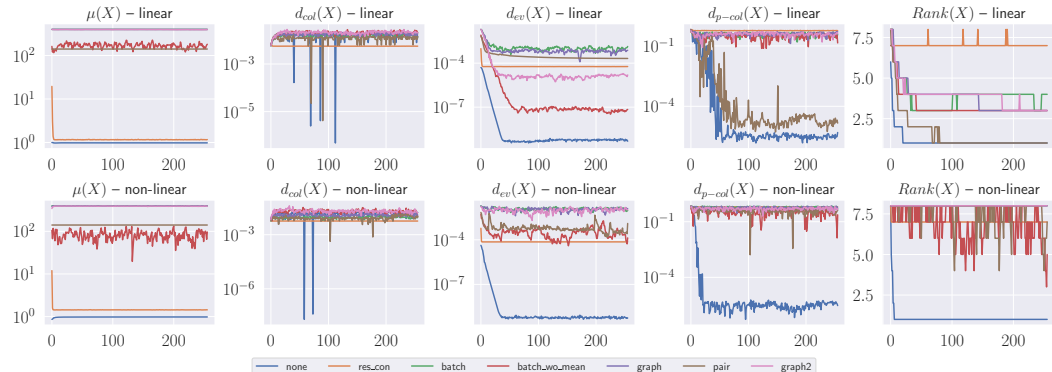


Figure 3: Long Term behavior of GIN. Progression of the above measures of convergence over 256 iterations of message-passing in both linear and non-linear GIN.

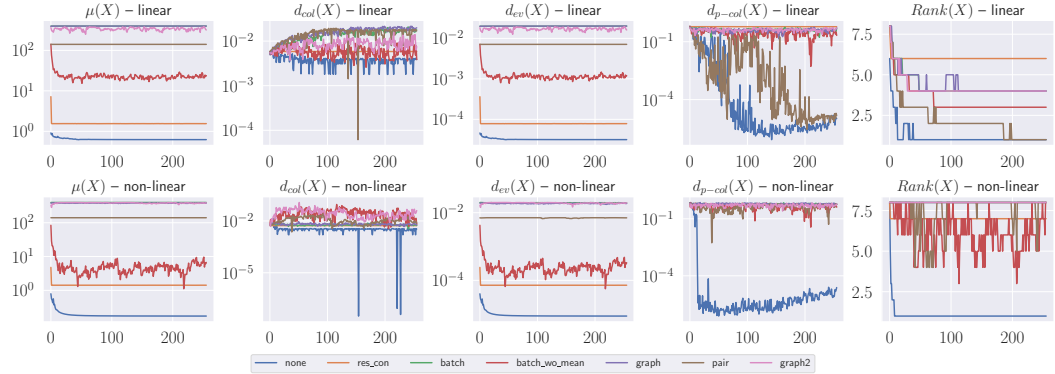


Figure 4: **Long Term behavior of GAT.** Progression of the above measures of convergence over 256 iterations of message-passing in both linear and non-linear GAT.

Datasets We provide summary statistics for datasets used in experiments in Section 6 in Table 2.

Table 2: The summary statistics of the datasets used in Section 6.

Dataset	#graphs	#nodes	#edges	#features	# classes
MUTAG	188	~17.9	~39.6	7	2
PROTEINS	1,113	~39.1	~145.6	3	2
PTC-MR	344	~14.29	~14.69	18	2
Cora	1	2,708	10,556	1,433	7
Citeseer	1	3,327	9,104	3,703	6
PubMed	1	19,717	88,648	500	3
ogbn-arxiv	1	169,343	1,166,243	128	40

Training details We perform a within-fold 90%/10% train/validation split for model selection. We train the models for 200 epochs using the AdamW optimizer and search the hyperparameter space over the following parameter combinations:

- learning rate $\in \{10^{-4}, 10^{-3}, 10^{-2}, 10^{-1}\}$
- feature size $\in \{32, 64\}$
- weight decay $\in \{0, 10^{-2}, 10^{-4}\}$
- number of layers $\in \{3, 5\}$

We select the hyperparameters of the model with the best mean validation accuracy over its 30 best epochs. The code and all non publicly available data will be made available here.

Compute We ran all of our experiments on a system with two NVIDIA L40 GPUs, two AMD EPYC 7H12 CPUs and 1TB RAM.

Licenses

- PyG [19]: MIT license
- OGB [25]: MIT license
- ogbn-arxiv: ODC-BY